J. Cell. Mol. Med. Vol 16, No 4, 2012 pp. 789-811

Transcriptional insights on the regenerative mechanics of axotomized neurons *in vitro*

Jian Ming Jeremy Ng [a, #], Minghui Jessica Chen [a, #], Jacqueline Y.K. Leung [a], Zhao Feng Peng [b, c], Jayapal Manikandan [d], Robert Z. Qi [e], Meng Inn Chuah [a], Adrian K. West [a], James C. Vickers [a], Jia Lu [f], Nam Sang Cheung [a, g, *], Roger S. Chung [a, *]

[a] *Menzies Research Institute, University of Tasmania, Hobart, Tasmania, Australia*
[b] *Key Laboratory of Biogeology and Environmental Geology of the Ministry of Education, China University of Geosciences, Wuhan, China*
[c] *Department of Biochemistry, Yong Loo Lin School of Medicine, National University of Singapore, Singapore*
[d] *Department of Physiology, Yong Loo Lin School of Medicine, National University of Singapore, Singapore*
[e] *Department of Biochemistry, State Key Laboratory of Molecular Neuroscience, The Hong Kong University of Science and Technology, Clear Water Bay, Kowloon, Hong Kong, China*
[f] *Defense Medical and Environmental Research Institute, DSO National Laboratories, National University of Singapore, Singapore*
[g] *School of Life and Environmental Sciences, Deakin University, Burwood, Melbourne, Australia*

Received: April 06, 2011; Accepted: June 12, 2011

Abstract

Axotomized neurons have the innate ability to undergo regenerative sprouting but this is often impeded by the inhibitory central nervous system environment. To gain mechanistic insights into the key molecular determinates that specifically underlie neuronal regeneration at a transcriptomic level, we have undertaken a DNA microarray study on mature cortical neuronal clusters maintained *in vitro* at 8, 15, 24 and 48 hrs following complete axonal severance. A total of 305 genes, each with a minimum fold change of ± 1.5 for at least one out of the four time points and which achieved statistical significance (one-way ANOVA, $P < 0.05$), were identified by DAVID and classified into 14 different functional clusters according to Gene Ontology. From our data, we conclude that post-injury regenerative sprouting is an intricate process that requires two distinct pathways. Firstly, it involves restructuring of the neurite cytoskeleton, determined by compound actin and microtubule dynamics, protein trafficking and concomitant modulation of both guidance cues and neurotrophic factors. Secondly, it elicits a cell survival response whereby genes are regulated to protect against oxidative stress, inflammation and cellular ion imbalance. Our data reveal that neurons have the capability to fight insults by elevating biological antioxidants, regulating secondary messengers, suppressing apoptotic genes, controlling ion-associated processes and by expressing cell cycle proteins that, in the context of neuronal injury, could potentially have functions outside their normal role in cell division. Overall, vigilant control of cell survival responses against pernicious secondary processes is vital to avoid cell death and ensure successful neurite regeneration.

Keywords: neurons • axotomy • microarray • regeneration • neurite cytoskeleton • secondary processes

Introduction

One of the striking features of the injured central nervous system (CNS) is the failure of severed axons to adequately regenerate to restore loss of function. This was initially believed to be caused by an intrinsic inability of injured axons to sprout regenerative processes. However, the seminal studies of Albert Aguayo and others using peripheral or cellular tissue grafts transplanted into the lesioned spinal cord have clearly demonstrated that the environment of the injured CNS is a critical determinant of whether injured axons can regenerate [1]. The molecular determinates of the inhibitory CNS environment are now well-understood, with major players being myelin-associated molecules (such as nogo, myelin-associated glycoprotein) and chondroitin sulphate proteoglycans [2].

Equally important has been the discovery that injured neurons have an intrinsic capacity to regenerate following complete axonal transection. Although bearing the limitation of being one-dimen-

[#]Both the authors contributed equally to this study.
*Correspondence to: Roger S. CHUNG, Steve Nam Sang CHEUNG, Menzies Research Institute, School of Medicine
Private Bag 23, University of Tasmania, Hobart,
Tasmania 7001, Australia.
Tel.: +613-6226 2657/2710
Fax: +613 6226 7704
E-mail: Roger.Chung@utas.edu.au, Nam.Cheung@utas.edu.au

doi:10.1111/j.1582-4934.2011.01361.x

sional, *in vitro* experimental models have proven particularly insightful in this field of research. A particular advantage of these approaches is the ability to specifically evaluate intrinsic regeneration of injured axons in the absence of glial cells or inhibitory substrates and molecules. Elegant studies have demonstrated that severance of individual axons of cultured CNS neurons results in a rapid regenerative response [3, 4]. Furthermore, axotomy of thick fasciculated axonal bundles of mature (21 days *in vitro*) clusters of cortical neurons results in regenerative sprouting within 8 hrs after injury [5, 6].

Several studies have directly investigated the precise mechanisms that underlie the intrinsic regenerative sprouting response of injured CNS neurons. Microtubule stabilizing drugs significantly alter the regenerative sprouting response following axonal transection of cortical neurons *in vitro*, indicating that cytoskeletal re-organization is a key process underlying axonal regeneration [6]. This has recently been confirmed by *in vivo* studies reporting that the microtubule stabilizing drug taxol facilitates axonal regeneration of the injured optic nerve [7]. Highlighting that the regenerative sprouting response is an active process, Verma *et al.* [8] have reported that protein synthesis is essential for efficient generation of regenerative growth cones following axotomy *in vitro*. They demonstrated that axotomy leads to a four- to six-fold increase in ^{3}H-leucine incorporation, and that the protein synthesis inhibitors cycloheximide and anisomycin both impair the ability of severed axons to form regenerative sprouts [8].

To identify key molecular determinants of successful axonal regeneration, a number of studies have utilized DNA microarray techniques to reveal groups of genes that are up- or down-regulated in response to axonal injury and during axonal regeneration. These studies have implicated a wide variety of genes in the regenerative response, including cytoskeletal, cell cycle and ion homeostasis genes. A notable feature of these studies is that they have generally been undertaken within *in vivo* injury situations, such as the injured optic nerve [9, 10], sciatic nerve [11, 12] or spinal cord [13, 14]. Hence, because of the presence of glia and other cells and the inability of microarray approaches to discriminate cell-specific gene expression, these studies do not give a clear indication of the key genes directly responsible for intrinsic regenerative sprouting of injured neurons. To address this, we have undertaken a microarray study following complete axonal severance of mature (21 days *in vitro*) cultured cortical neurons.

Materials and methods

Cell culture preparation for rat primary cortical neuronal clusters

All animal experimentation was performed under the guidelines stipulated by the University of Tasmania Animal Ethics Committee, which is in accordance with the Australian code of practice for the care and use of animals for scientific purposes. Cortical neuron cultures were prepared according to previously published protocols [6, 15, 16]. Briefly, cortical tissue was isolated from E17 hooded Wistar rat embryos and incubated in 0.1% trypsin (in HEPES buffer) for 15 min. Following trituration and filtration through a 20 μm filter, neurons were plated into 12-well tissue culture plates pre-coated overnight with 1mg/ml of L-lysine in borate buffer, pH 7.4, at a cell density of 4.5×10^5 cells/well. Neuronal cultures were maintained at 37°C in humidified air containing 5% CO_2 for 21 days before experimental axotomy. Neurons were initially plated into a culture medium consisting of Neurobasal™ medium (Gibco; Life Technologies Corp., California, USA), supplemented with 10% foetal bovine serum, 0.1% B-27 supplement (Gibco), 0.1 mM L-glutamine (Gibco) and 200 U/ml gentamicin (Gibco). After 24 hrs, the media was replaced with medium lacking foetal bovine serum, and replaced every 3 or 4 days.

Axotomy of rat primary cortical neuronal clusters

Neurons were maintained in culture for 21 days, at which time they had formed large spherical clusters of neurons and an interconnected network of thick fasciculated bundles of axons. Using a fine blade microscalpel, axonal bundles were completely severed at approximately half way along the axonal bundles. All axonal bundles in each culture well were severed. At the appropriate time points, RNA from neuronal cells were collected, representing neurons both proximal and distal to the axotomy.

Total RNA extraction and isolation

RNA from neuronal clusters was extracted at indicated time points (8, 15, 24 and 48 hrs) after axotomy and control (no axotomy) using RNeasy Mini Kit (Qiagen Cat. No. 74104) as per the manufacturer's instructions. The whole procedure was performed with RNase-free filtered pipette tips. 1.5 μl of the RNA sample was taken for spectrophotometric quantification using Nanodrop ND-1000 Version 3.2.1. Another 1 μl was used for RNA quality analysis using E-gene HDA-GT12 genetic analyser.

Real-time (RT)-PCR

Reverse transcription was carried out according to steps specified by manufacturer (Applied Biosystems Taqman reverse transcription reagents; Life Technologies Corp.). Each cDNA sample was duplicated with two No Template Control (NTC) for each probe used. All genes tested were normalized against either of the internal loading controls, 18S rRNA or GAPDH. Twenty microlitres of the Taqman master mix was pipetted to the bottom of each well of the optical 96-well fast reaction plate. Five microlitres of cDNA or water (NTC) was added to the designated reaction well. The plate was then read by the 7000 Fast Real-Time PCR System with conditions according to the manufacturer's protocol.

DNA microarray

Transcriptomic profiling was performed on Illumina Rat Ref12 Ver.1 arrays for rat neuronal clusters 8, 15, 24 and 48 hrs after axonal sever-

ance. Six biological replicates were obtained for the control and three for each of the four time-points after injury. Five hundred nanograms of total RNA for each sample was brought up to an initial volume of 11 μl. RNA reverse transcription was performed with Illumina® TotalPrep RNA Amplification Kit and the concentration of cRNA was quantitated using the NanoDrop ND-1000. Seven hundred and fifty nanograms of cRNA topped up to 5 μl RNase-free water was mixed with 10 μl hybridization buffer. Hybridization using streptavidin-Cy3 labelling was carried out according to the manufacturer's instruction (Illumina Inc., San Diego, USA). Subsequently, the beadchip was read on the Illumina scanner using Bead Studio software at Scan Factor = 0.65.

Microarray data collection and analysis

Analysis of the scanned images was performed with BeadScan (Illumina Inc.). Signal data generated from the Illumina®Bead Studio software was analysed using GeneSpring© v7.3 software. All differentially expressed genes in this study were selected based on the following parameters: (1) a minimum of ±1.5 fold change in at least one of post-injury time-points and (2) passed the statistical screening test of one-way ANOVA ($P < 0.05$) and Benjamini-Hochberg False Discovery Rate Correction. Genes which were differentially expressed were annotated according to Gene Ontology Biological process with the use of an online bioinformatics resource namely Database for Annotation, Visualization and Integrated Discovery (DAVID) 6.7 (http://david.abcc.ncifcrf.gov/) [17, 18]. All microarray data reported here are described in accordance with MIAME guidelines, and have been deposited in NCBIs Gene Expression Omnibus (GEO; http://www.ncbi.nlm.nih.gov/geo/) and are accessible through GEO Super-Series accession number GSE 23653.

Statistical analysis

All experiments were repeated at least three times. Data were analysed using *post-hoc* Tukey test with one-way ANOVA to assess significant differences in multiple comparisons. Values of $P < 0.05$ were considered as statistically significant and presented as mean ± S.E.

Results

DNA microarray analysis

Gene expression profiles were obtained for 8, 15, 24 and 48 hrs post severance of axon bundles connecting rat neuronal clusters in culture. Genes with a minimum fold change of ±1.5 for at least one of the four time points were classified as differentially regulated and subjected to one-way ANOVA analysis. Those that reached significance with a $P < 0.05$ were subjected to grouping using the online bioinformatics resource DAVID. A total of 305 genes were identified and each of them was then classified into one out of the 14 functional clusters identified to avoid overestimation (Table 1). Figure 1 summarizes the number of identified genes in each biological process and the percentage these genes within the group occupied out of the total. Differences between up and down regulated genes across the four time points after axotomy were presented in Figure 2A and B, respectively. Generally, even though the genomic profiles across time were quite similar, it was evident from Figure 2A that there was a slight transient elevation of genes involved in certain biological processes such as axogenesis, morphogenesis, actin and cytoskeleton organization, cell cycle, response to oxidative stress, inflammation and chemotaxis at 8 hrs in comparison to the later time points and this was conversely true for the down-regulated genes as seen in Figure 2B.

Association of genes with biological processes

Neurite network associated genes

There was a down-regulation of genes responsible for repulsive axon guidance cues and their receptors that are known to limit axonal regeneration and these include *Efn*, *Sema*, *Slit*, *Bmp*, *Nrp*, *Plxd* and *Eph*. Conversely, there was an increased expression of neurite outgrowth promoting genes such as *Apoe*, *Cntf*, *Vgf* and *Lama5*. In addition, there was a transient elevation in gene expression at 8 hrs that faltered with time for *Snap*, *Tnn* and neurotrophic-associated factors such as *Nrtk* and *Bdnf*. A varied expression of genes involved in actin filament formation and microtubule organization was observed and they include *Tuba*, *Tubb*, *Acta*, *Actb*, *Spnb*, *Pfn*, *Stmn*, *Arp2/3*, *N-WASP* and *Map1b*. Our data also reflected on the importance of protein trafficking during axonal repair as genes known to facilitate this process, mainly motor (*Dnc*, *Dna*, *Kif*, *Myh*, *Tpm*) and vesicle proteins (*Vamp*, *Syt*, *Snap*) were also differentially expressed.

Oxidative insult-related genes

Transcriptomic data revealed an elevated expression of genes related to GSH biosynthesis namely *Gstm1*, *Mgst1*, *Gss* and *Gpx1*. This was accompanied by a brief expression of *Txnrd1* at 8 hrs and a prolonged expression of antioxidant enzyme genes which include superoxide dismutase (*Sod2* and *Sod3*) and peroxiredoxin (*Prdx6*). Moreover, heat shock proteins (*Hspa2*, *Hspb1*, *Hspb8*, *Hspb6*, *Hspca*), that serve as molecular chaperones were also significantly up-regulated (except *Hspa5*).

Cell cycle and death genes

There was a diminished expression of various pro-apoptosis genes such as *Apaf1* and *Casp 3*, *11 and 12* with the exception of *Csap6*. In addition, *Bnips*, a group of pro-apoptosis *Bcl-2* family proteins, were also significantly down-regulated. Accordingly, increased gene expression of *Rap1a* and *Braf* might represent activation of MEK/ERK pro-survival signalling pathway. Intriguingly, a series of cell cycle proteins were differentially regulated and some examples of which include *Aurkb*, a range of cyclins and few tran-

Table 1 Gene profiles of neuronal clusters *in vitro*, 8, 15, 24 and 48 hrs after axon severance ($P < 0.05$)

GenBank	Symbols	Gene name	Time							
			8 hrs	S.E. (±)	15 hrs	S.E. (±)	24 hrs	S.E. (±)	48 hrs	S.E. (±)
Regulation of axonogenesis										
NM_013191	S100b	S100 protein, , polypeptide	6.57	2.62	7.94	2.10	5.81	2.44	8.52	2.37
NM_013166	Cntf	Ciliary neurotrophic factor	4.06	1.73	5.76	1.75	4.33	2.04	5.30	3.02
NM_012809	Cnp1	Cyclic nucleotide phosphodiesterase 1	2.52	1.83	3.69	1.28	2.87	1.39	3.44	1.01
NM_138828	Apoe	Apolipoprotein E	2.00	0.54	2.30	0.69	2.27	0.68	2.28	0.81
XM_236640	Plxnb1	Plexin B1 (predicted)	1.96	0.63	2.53	0.71	2.23	0.68	2.15	0.57
NM_017026	Mbp	Myelin basic protein	1.85	1.42	2.40	1.34	1.48	0.44	2.11	0.68
NM_013001	Pax6	Paired box gene 6	1.81	0.52	1.80	0.50	1.70	0.50	1.88	0.62
NM_199407	Unc5c	Unc-5 homologue C	1.79	0.56	1.75	0.49	1.46	0.43	1.35	0.41
NM_012829	Cck	Cholecystokinin	1.78	1.59	−2.05	0.98	1.37	1.99	−1.32	0.91
NM_031066	zygin I,Fez1	Fasciculation and elongation protein ·	1.51	0.41	1.58	0.47	1.73	0.46	1.59	0.63
NM_181086	Tnfrsf12a	Tumour necrosis factor receptor superfamily, member 12a	1.46	0.43	−1.56	0.21	−1.18	0.50	−1.67	0.29
XM_217250	Ephb1	Eph receptor B1	1.40	0.46	2.31	0.67	1.85	0.63	1.40	0.46
XM_236203	Dscaml1	Down syndrome cell adhesion molecule-like 1 (predicted)	1.29	0.40	1.60	0.54	1.37	0.44	1.21	0.35
XM_222794	Tnn	Tenascin N (predicted)	1.19	1.18	−1.30	0.22	−1.22	0.34	−1.54	0.19
NM_012934	Dpysl3	Dihydropyrimidinase-like 3	−1.38	0.22	−1.67	0.20	−2.10	0.17	−2.14	0.12
NM_012610	Ngfr	Nerve growth factor receptor (member 16)	−1.38	0.18	−1.57	0.18	−1.62	0.16	−1.31	0.24
XM_341201.2	Epha5	Eph receptor A5 (predicted)	−1.39	0.40	−3.12	0.19	−2.06	0.29	−2.74	0.10
NM_023023	Dpysl5	Dihydropyrimidinase-like 5	−1.44	0.22	−1.72	0.18	−1.55	0.27	−1.92	0.17
NM_019272	Sema4f	Semaphorin 4f	−1.46	0.32	−2.56	0.34	−1.62	0.46	−2.74	0.32
NM_017310	Sema3a	Short basic domain, secreted, semaphorin 3A	−1.68	0.20	−1.84	0.17	−1.65	0.17	−1.73	0.17
NM_031073	Ntf3	Neurotrophin 3	−1.69	0.16	−1.73	0.18	−1.66	0.17	−1.80	0.16
XM_236623	Sema3f	Short basic domain, secreted, semaphorin 3 F (predicted)	−1.81	0.16	−1.99	0.18	−2.22	0.12	−1.89	0.16
XM_234514	Bcl11b	B-cell leukaemia/lymphoma 11B (predicted)	−1.85	0.41	−3.78	0.24	−2.53	0.37	−4.01	0.26
NM_019288	App	Amyloid , (A4) precursor protein	−2.38	0.11	−2.59	0.12	−2.85	0.11	−2.89	0.14
XM_341567.2	Plxdc2	Plexin domain containing 2 (predicted)	−2.40	0.15	−1.62	0.19	−2.54	0.24	−2.04	0.23
NM_145098	Nrp1	Neuropilin 1	−2.55	0.13	−4.53	0.06	−3.78	0.08	−3.82	0.09
NM_053485	S100a6	S100 calcium binding protein A6 (calcyclin)	−5.71	0.05	−5.76	0.05	−6.93	0.04	−6.74	0.04

Continued

Table 1 Continued

GenBank	Symbols	Gene name	Time							
			8 hrs	S.E. (±)	15 hrs	S.E. (±)	24 hrs	S.E. (±)	48 hrs	S.E. (±)
Neurite development and morphogenesis										
XM_215963	Lama5	Laminin, ·5	2.39	0.73	2.21	0.75	2.05	0.56	1.88	0.54
XM_342392	Notch1	Notch gene homologue 1,	2.35	0.65	2.43	0.64	2.00	0.55	1.81	0.48
NM_030997.1	Vgf	VGF nerve growth factor inducible	2.25	0.58	1.42	0.40	1.71	0.64	1.15	0.35
NM_053021	Clu	Clusterin	1.96	0.61	2.17	0.68	1.89	0.68	2.43	0.73
NM_053911	Pscd2	Pleckstrin homology, Sec7 and coiled/coil domains 2	1.77	0.53	1.64	0.49	1.70	0.53	1.45	0.67
XM_221672	Tiam1	T cell lymphoma invasion and metastasis 1 (predicted).	1.66	0.60	−1.07	0.46	1.20	0.71	−1.14	0.52
NM_031131	Tgfb2	Transforming growth factor, ,2	1.58	0.60	1.13	0.67	1.08	0.39	1.04	0.72
NM_012924	Cd44	CD44 antigen	1.58	0.47	−1.08	0.28	−1.02	0.53	−1.11	0.40
NM_030991	Snap25	Synaptosomal-associated protein 25	1.18	0.93	−2.69	0.65	−1.00	1.52	−2.46	0.80
NM_019248	Ntrk3	Neurotrophic tyrosine kinase, receptor, type 3	1.06	0.46	−1.33	0.23	−1.18	0.27	−1.56	0.21
NM_012731	Ntrk2	Neurotrophic tyrosine kinase, receptor, type 2	1.03	0.32	−2.14	0.17	−1.27	0.44	−2.15	0.37
NM_012513	Bdnf	Brain-derived neurotrophic factor	1.01	0.68	−1.84	0.17	−1.24	0.51	−1.79	0.15
NM_012700.1	Stx1b	Syntaxin 1B2 (2)	−1.00	0.27	−1.41	0.31	−1.03	0.42	−1.51	0.35
XM_232283	Plxnb1	Plexin D1 (predicted)	−1.05	0.25	−1.30	0.22	−1.19	0.24	−1.65	0.18
NM_153470	Lzts1	Leucine zipper, putative tumour suppressor 1	−1.12	0.73	−2.09	0.51	−1.17	0.81	−2.02	0.47
NM_013038	Stxbp1	Syntaxin binding protein 1	−1.20	0.54	−2.54	0.37	−1.47	0.66	−2.62	0.35
NM_133652	Cspg5	Chondroitin sulphate proteoglycan 5	−1.28	0.22	−1.59	0.19	−1.55	0.21	−1.30	0.37
XM_579472	Slit1	Slit homologue 1	−1.53	0.30	−2.35	0.30	−1.56	0.45	−2.91	0.17
NM_019334	Pitx2	Paired-like homeodomain transcription factor 2	−1.53	0.18	−1.54	0.20	−1.54	0.19	−1.44	0.19
NM_017237	Uchl1	Ubiquitin carboxy-terminal hydrolase L1	−1.60	0.35	−2.32	0.27	−1.75	0.32	−2.56	0.31
NM_012548	Edn1	Endothelin 1	−1.61	0.19	−1.78	0.21	−1.80	0.16	−1.71	0.17
NM_134331	Epha7	Eph receptor A7	−1.65	0.18	−1.53	0.22	−1.52	0.23	−1.52	0.20
XM_346464	Slit2	Slit homologue 2	−1.69	0.17	−1.56	0.18	−1.83	0.17	−1.88	0.22
XM_342172	Thbs4	Thrombospondin 4	−1.70	0.16	−1.74	0.19	−1.95	0.15	−2.19	0.12
XM_223820	Zfp312	Zinc finger protein 312 (predicted)	−1.79	0.47	−3.76	0.13	−1.55	0.64	−3.10	0.10
XM_215451	Cspg2	Chondroitin sulfate proteoglycan 2	−1.80	0.22	−1.38	0.22	−1.94	0.17	−2.11	0.16
XM_342591	Bmp7	Bone morphogenetic protein 7	−2.12	0.25	−1.27	0.23	−1.76	0.32	1.22	0.58
NM_017089	Efnb1	Ephrin B1	−2.56	0.10	−2.94	0.14	−2.86	0.10	−3.15	0.08
NM_031321	Slit3	Slit homologue 3	−2.84	0.11	−3.26	0.10	−3.19	0.09	−3.52	0.08
NM_053595	Pgf	Placental growth factor	−5.49	0.05	−4.06	0.08	−5.27	0.06	−4.70	0.06
NM_012774	Gpc3	Glypican 3	−9.15	0.10	−4.92	0.06	−9.44	0.04	−5.87	0.05

Continued

Table 1 Continued

GenBank	Symbols	Gene name	Time							
			8 hrs	S.E. (±)	15 hrs	S.E. (±)	24 hrs	S.E. (±)	48 hrs	S.E. (±)
Actin filament formation										
XM_341553	PRKCQ	Protein kinase C, theta	3.84	1.86	5.17	1.56	4.04	2.02	4.55	1.39
XM_342648.2	N-WASP	Neural Wiskott--Aldrich syndrome protein	3.75	1.28	4.83	1.64	3.53	2.07	4.24	2.38
XM_218617.3	Myh14	Myosin, heavy polypeptide 14 (predicted)	2.96	0.70	3.44	0.99	2.87	0.87	2.51	1.06
NM_019357	Vil2	Villin 2	2.16	0.67	1.57	0.46	1.66	0.41	1.73	0.58
NM_053484	Gas7	Growth arrest specific 7	2.15	0.96	1.14	0.75	1.65	1.52	1.10	0.54
NM_019131	Tpm1	Tropomyosin 1, α	1.94	0.58	2.03	0.64	1.76	0.47	1.84	0.94
NM_017117.1	Capn3	Calpain 3	1.7	0.5	1.89	0.62	1.49	0.49	1.53	0.42
NM_022401.1	Plec1	Plectin 1	1.68	0.42	1.72	0.51	1.43	0.37	1.18	0.40
NM_001005889	Rdx	Radixi	1.61	0.46	1.61	0.54	1.40	0.46	1.29	0.66
NM_019167	Spnb3	β-Spectrin 3	1.45	1.17	−1.73	0.69	1.22	1.53	−1.91	0.56
XM_221196	Fscn2	Fascin homologue 2, actin-bundling protein (predicted)	1.20	0.39	1.32	0.45	1.30	0.43	1.58	0.52
XM_236444.3	LOC315840	Similar to Myosin VI	1.17	0.33	1.59	0.43	1.36	0.43	1.29	0.40
NM_030873	Pfn2	Profilin 2	−1.06	0.24	−1.31	0.22	−1.14	0.24	−1.58	0.34
XM_237115	Nck2	Non-catalytic region of tyrosine kinase adaptor protein 2	−1.08	0.39	−1.72	0.30	−1.36	0.35	−1.74	0.32
NM_031144	Actb	Actin, β	−1.30	0.24	−1.36	0.24	−1.59	0.21	−1.44	0.36
XM_579522	Actn4	Actinin ·4	−1.31	0.22	−1.65	0.17	−1.81	0.17	−1.75	0.18
NM_013194	Myh9	Myosin, heavy polypeptide 9	−1.35	0.25	−1.59	0.17	−1.66	0.18	−1.42	0.20
XM_215862	Dstn	Destrin (predicted)	−1.38	0.22	−1.34	0.28	−1.64	0.21	−1.55	0.37
NM_001009689	Cdc42ep2	CDC42 effector protein (Rho GTPase binding) 2	−1.54	0.18	−1.59	0.20	−1.83	0.16	−1.74	0.16
NM_019289.2	Arpc1b	Actin-related protein 2/3 complex, subunit 1B	−1.61	0.16	−1.70	0.17	−1.81	0.15	−1.92	0.16
NM_053814	Mrip	Myosin phosphatase-Rho interacting protein	−1.64	0.17	−2.16	0.13	−2.43	0.13	−2.78	0.14
XM_579484	Evl	Ena-vasodilator stimulated phosphoprotein	−1.79	0.14	−2.45	0.14	−1.96	0.19	−2.88	0.17
NM_019212	Acta1	Actin, α1, skeletal muscle	−1.91	0.16	−2.27	0.40	−2.22	0.21	−2.49	0.42
NM_023992	Gpr54	G protein-coupled receptor 54	−2.05	0.16	−2.10	0.13	−2.01	0.15	−2.07	0.14
XM_579179	Arhe	Ras homologue gene family, member E	−2.21	0.13	−2.45	0.13	−2.45	0.13	−2.62	0.14
NM_001007554	Cal	CSX-associated LIM	−4.19	0.08	−4.57	0.06	−4.66	0.07	−3.90	0.08
NM_012722	Eln	Elastin	−4.62	0.12	−3.69	0.12	−4.63	0.09	−3.98	0.08
NM_012893.1	Actg2	Actin, γ2	−33.7	0.01	−28.1	0.01	−22.3	0.03	−26.5	0.01

Continued

Table 1 Continued

GenBank	Symbols	Gene name	Time							
			8 hrs	S.E. (±)	15 hrs	S.E. (±)	24 hrs	S.E. (±)	48 hrs	S.E. (±)
Microtubule cytoskeleton organization and biogenesis										
XM_341694.2	Dncl2b	Dynein, cytoplasmic, light chain 2B (predicted)	20.8	6.64	23.8	7.22	16.4	13.4	22.5	10.6
NM_053508	Tekt1	Tektin 1	6.81	2.11	8.84	2.55	6.01	4.81	8.01	4.91
NM_001007726	Dnai2	Dynein, axonemal, intermediate polypeptide 2	6.65	2.05	8.07	2.65	5.66	3.42	6.58	3.78
XM_224615.3	Dnah1	Dynein, axonemal, heavy polypeptide 1	4.83	1.30	7.20	2.05	5.82	3.20	5.22	2.69
XM_576475.1	vOC501059	Similar to kinesin-like protein 9	2.52	0.78	2.70	0.77	2.35	0.96	2.72	0.86
NM_012935	Cryab	Crystallin, ·B	2.44	1.35	2.33	0.88	2.12	0.65	2.03	1.25
XM_234720.3	Dnah11	Dynein, axonemal, heavy polypeptide 11	2.41	0.67	3.06	0.86	2.37	0.80	2.56	0.80
XM_213354.3	Dnah9	Dynein, axonemal, heavy polypeptide 9	2.02	0.67	2.45	0.82	2.03	0.82	2.30	0.79
NM_001007004	Tuba4	Tubulin, ·4	1.97	0.59	1.03	0.31	1.53	0.64	−1.08	0.52
NM_199094.1	Tubb2	Tubulin, ,2	1.96	0.57	1.81	0.54	1.77	0.58	1.74	0.56
NM_206950	Mig12	MID1 interacting G12-like protein	1.96	0.52	2.20	0.66	2.00	0.53	1.94	0.69
XM_575908	Tekt2	Tektin 2 (predicted)	1.92	0.56	2.07	0.62	1.66	0.87	2.32	0.68
NM_031763	Pafah1b1	Platelet-activating factor acetylhydrolase, isoform Ib	1.74	0.46	1.76	0.55	1.58	0.43	1.56	0.39
XM_218820	Prc1	Protein regulator of cytokinesis 1 (predicted)	1.65	0.48	1.46	0.43	1.43	0.37	1.63	0.79
NM_001009666	Dnalc4	Dynein, axonemal, light chain 4	1.56	0.46	1.43	0.36	1.28	0.42	1.24	0.51
NM_001009645	Kif22	Kinesin family member 22	1.53	0.39	1.06	0.31	1.16	0.31	1.17	0.50
XM_240978.3	Kifc3	Kinesin family member C3 (predicted)	1.50	0.41	1.50	0.38	1.65	0.47	1.06	0.32
XM_341686	Ap1g1	Adaptor-related protein complex 1, gamma 1 subunit	1.49	0.42	1.41	0.51	1.51	0.43	1.21	0.44
NM_053618	Bbs2	Bardet--Biedl syndrome 2 homologue	1.45	0.37	1.58	0.48	1.44	0.43	1.44	0.45
XM_224232	Cenpj	Centromere protein J	1.33	0.38	1.51	0.43	1.33	0.45	1.32	0.41
NM_022507	Prkcz	Protein kinase C, zeta	1.00	0.28	−1.36	0.26	−1.11	0.40	−1.60	0.35
NM_198752.1	KIFC2	Kinesin family member C2	−1.01	0.36	−2.00	0.38	−1.26	0.74	−2.40	0.27
NM_053947	Mark1	MAP/microtubule affinity-regulating kinase 1	−1.11	0.25	−1.55	0.22	−1.34	0.25	−1.80	0.17
XM_343018.2	Spg4	Spastic paraplegia 4 (spastin) (predicted)	−1.25	0.23	−1.38	0.21	−1.43	0.19	−1.68	0.25
NM_024346	Stmn3	Stathmin-like 3	−1.43	0.37	−2.39	0.30	−1.56	0.48	−2.66	0.28
NM_133320	Ndel1	nudE nuclear distribution gene E homologue like 1	−1.60	0.18	−2.32	0.12	−1.79	0.20	−2.55	0.20
XM_215469	Map1b	Microtubule-associated protein 1b	−1.63	0.35	−2.22	0.18	−2.12	0.23	−2.74	0.17
NM_017166	Stmn1	Stathmin 1	−2.11	0.25	−2.84	0.21	−2.29	0.28	−3.10	0.17

Continued

Table 1 Continued

GenBank	Symbols	Gene name	Time 8 hrs	S.E. (±)	15 hrs	S.E. (±)	24 hrs	S.E. (±)	48 hrs	S.E. (±)
Apical protein localization										
XM_223229	Shrm	PDZ domain actin binding protein Shroom	1.67	0.52	1.74	0.57	1.45	0.53	1.55	0.48
XM_222896	Ltap	Loop tail associated protein (predicted)	1.41	0.52	1.48	0.35	1.23	0.54	1.33	0.55
Cell cycle										
NM_053749	Aurkb	Aurora kinase B	4.99	1.95	5.90	1.71	4.01	1.58	5.80	1.65
XM_574943	Ccna1	Cyclin A1 (predicted)	3.94	1.18	4.67	1.39	3.01	1.56	3.69	1.88
XM_573172	Pnutl2	Peanut-like 2 (predicted)	3.33	1.34	3.48	1.10	2.47	1.18	2.79	2.11
XM_579390	Hrasls3	HRAS-like suppressor	3.29	1.20	4.37	1.23	3.32	1.57	4.59	1.43
XM_220423	Sept8	Septin 8 (predicted)	2.40	1.16	1.88	1.06	2.26	1.05	1.71	1.41
NM_053677	Chek2	Protein kinase Chk2	2.33	0.84	2.58	0.75	1.91	0.70	2.45	1.03
NM_021863	Hspa2	Heat shock protein 2	2.17	0.64	2.09	0.59	1.62	0.48	2.12	0.74
XM_215222	Cetn2	Centrin 2	2.15	0.60	2.43	0.71	1.97	0.81	2.15	1.16
XM_574892	E2f5	E2F transcription factor 5	1.86	0.54	1.54	0.45	1.69	0.51	1.44	0.45
NM_001005765	Rap1a	RAS-related protein 1a	1.76	0.54	1.65	0.45	1.49	0.49	1.49	0.41
XM_579383	vOC501059	Adenylate cyclase activating polypeptide 1	1.74	1.96	−1.90	0.30	1.14	2.35	−2.01	0.25
NM_001004107	Tacc1a	Transforming, acidic coiled-coil containing protein 1a	1.58	0.47	1.51	0.42	1.48	0.40	1.20	0.47
NM_133396	Tesk2	Testis-specific kinase 2	1.50	0.44	1.34	0.40	1.35	0.40	1.33	0.36
NM_138873	Nbn	Nibrin	1.50	0.49	1.26	0.32	1.37	0.42	1.16	0.37
NM_013058	Id3	inhibitor of DNA binding 3	1.21	0.31	1.53	0.40	1.44	0.41	1.30	0.35
XM_579239	RT1-CE7	RT1 class I, CE7	1.20	0.37	1.62	0.70	1.09	0.29	1.39	0.42
NM_021739	Camk2b	Calcium/calmodulin-dependent protein kinase II ,subunit	1.16	0.51	−2.35	0.33	−1.22	0.73	−2.37	0.43
XM_341907	Eif4g2	Eukaryotic translation initiation factor 4, gamma 2	−1.16	0.28	−1.35	0.26	−1.56	0.21	−1.32	0.38
XM_342804	Ccne2	Cyclin E2 (predicted)	−1.40	0.20	−1.50	0.19	−1.51	0.21	−1.39	0.21
XM_222157	Kntc1	Kinetochore associated 1 (predicted)	−1.41	0.24	−1.50	0.26	−1.52	0.19	−1.68	0.18
XM_214152	Cdkn3	Cyclin-dependent kinase inhibitor 3 (predicted)	−1.47	0.21	−1.70	0.20	−1.95	0.15	−1.76	0.25
NM_053653	Vegfc	Vascular endothelial growth factor C	−1.48	0.29	−1.73	0.20	−1.61	0.20	−1.77	0.31
XM_223270	Ccng2	Cyclin G2 (predicted)	−1.53	0.19	−1.47	0.21	−1.57	0.20	−1.39	0.22
NM_053703	Map2k6	Mitogen-activated protein kinase kinase 6	−1.66	0.18	−1.51	0.17	−1.46	0.20	−1.82	0.19
NM_021693	Snf1lk	SNF1-like kinase	−1.67	0.27	−2.16	0.15	−1.84	0.33	−3.06	0.08
NM_139087	Cgref1	Cell growth regulator with EF hand domain 1	−1.69	0.23	−2.70	0.12	−1.86	0.27	−2.54	0.11
NM_052807	Igf1r	Insulin-like growth factor 1 receptor	−1.81	0.17	−2.06	0.16	−2.08	0.14	−2.52	0.11
NM_033099	Ptprv	Protein tyrosine phosphatase, receptor type, V	−2.37	0.11	−1.77	0.21	−2.19	0.14	−2.29	0.12
NM_053713.1	Klf4	Kruppel-like factor 4	−3.30	0.15	−3.81	0.10	−3.45	0.09	−4.09	0.10

Continued

Table 1 Continued

GenBank	Symbols	Gene name	Time 8 hrs	S.E. (±)	15 hrs	S.E. (±)	24 hrs	S.E. (±)	48 hrs	S.E. (±)
Negative regulation of programmed cell death										
NM_053819	Timp1	Inhibitor of metalloproteinase 1	1.79	0.51	1.83	0.53	1.46	0.43	1.13	0.30
XM_235497	Mkl1	Megakaryoblastic leukaemia (translocation) 1 (predicted)	1.05	0.27	−1.25	0.26	−1.09	0.31	−1.68	0.27
NM_033230	Akt1	Thymoma viral proto-oncogene 1	−1.20	0.26	−1.50	0.24	−1.43	0.23	−1.49	0.30
NM_207592	Gpi	Glucose phosphate isomerase	−1.34	0.19	−1.44	0.19	−1.37	0.21	−1.59	0.22
NM_031345	Dsipi	Delta sleep inducing peptide, immunoreactor	−1.37	0.21	−1.40	0.21	−1.69	0.18	−1.68	0.33
XM_216377	Bag1	Bcl2-associated athanogene 1 (predicted)	−1.48	0.20	−1.44	0.19	−1.53	0.20	−1.84	0.21
NM_057130.1	Bid3	BH3 interacting (with BCL2 family) domain	−1.58	0.18	−2.35	0.31	−1.74	0.27	−2.44	0.22
NM_013083	Hspa5	Heat shock 70 kD protein 5	−1.64	0.16	−1.51	0.17	−1.50	0.19	−1.74	0.24
XM_225257	Txndc5	Thioredoxin domain containing 5 (predicted)	−1.69	0.15	−1.52	0.21	−1.67	0.16	−1.52	0.21
NM_012992	Npm1	Nucleophosmin 1	−1.72	0.16	−2.25	0.16	−2.19	0.13	−2.35	0.18
NM_021691	Twist2	twist homologue 2	−2.47	0.12	−2.30	0.16	−2.63	0.10	−2.39	0.12
XM_225940	Tnfaip8	Tumour necrosis factor, α-induced protein 8 (predicted)	−3.13	0.09	−2.37	0.14	−3.10	0.09	−2.70	0.11
Regulation of apoptosis										
NM_031970	Hspb1	Heat shock 27 kD protein 1	3.35	1.04	4.01	1.24	3.34	1.33	4.61	1.37
NM_001007617	SNF1/AMPK	SNF1/AMP-activated protein kinase	2.97	1.47	3.44	1.10	2.96	1.35	3.28	2.28
NM_031775	Casp6	Caspase 6	2.13	0.80	2.61	0.78	2.00	0.73	2.64	1.00
NM_017180	Phlda1	Pleckstrin homology-like domain, family A, member 1	1.94	0.78	1.22	0.34	1.48	0.52	1.23	0.34
XM_231692	Braf	v-raf murine sarcoma viral oncogene homologue B1	1.69	0.52	1.98	0.70	1.63	0.52	1.57	0.70
NM_139261.1	Hspbp1	hsp70-interacting protein	1.68	0.51	1.39	0.45	1.54	0.45	1.26	0.72
NM_001004199	Tax1bp1	Tax1 (human T cell leukaemia virus type I) binding protein 1	1.41	0.38	1.67	0.54	1.42	0.43	1.31	0.41
XM_579385	G6pdx	Glucose-6-phosphate dehydrogenase	1.37	0.35	1.57	0.48	1.51	0.44	1.32	0.46
NM_012660	Eef1a2	Eukaryotic translation elongation factor 1 α2	1.16	0.63	−2.50	0.53	−1.10	0.94	−2.26	0.69
XM_217191	Bnip2	BCL2/adenovirus E1B 19kDa-interacting protein 1, NIP2	−1.24	0.25	−1.30	0.26	−1.48	0.23	−1.53	0.29
NM_012922	Casp3	Caspase 3, apoptosis related cysteine protease	−1.35	0.19	−1.47	0.19	−1.39	0.19	−1.51	0.21
NM_023979	Apaf1	Apoptotic peptidase activating factor 1	−1.40	0.21	−1.68	0.18	−1.52	0.20	−1.66	0.17
NM_080897	Bnip1	BCL2/adenovirus E1B 19 kD-interacting protein 1	−1.54	0.18	−1.81	0.15	−1.70	0.16	−2.00	0.15
NM_053420	Bnip3	BCL2/adenovirus E1B 19 kD-interacting protein 3	−1.62	0.17	−2.19	0.15	−2.10	0.14	−2.27	0.18
NM_053736	Casp11	Caspase 11	−2.31	0.14	−2.00	0.16	−2.46	0.13	−2.50	0.12
NM_130422	Casp12	Caspase 12	−2.54	0.12	−1.89	0.19	−2.52	0.12	−2.22	0.12
NM_172336	Atf5	Activating transcription factor 5	−2.62	0.15	−2.17	0.15	−2.14	0.20	−3.14	0.08

Continued

Table 1 Continued

GenBank	Symbols	Gene name	Time							
			8 hrs	S.E. (±)	15 hrs	S.E. (±)	24 hrs	S.E. (±)	48 hrs	S.E. (±)
Response to oxidative stress										
NM_017014	Gstm1	Glutathione S-transferase, Ì1	4.46	1.35	5.22	1.76	4.07	2.04	5.46	1.62
NM_012580	Hmox1	Heme oxygenase (decycling) 1	4.10	2.56	1.71	0.88	2.12	1.09	1.16	0.52
NM_134349	Mgst1	Microsomal glutathione S-transferase 1	2.90	0.87	3.39	1.00	3.08	1.07	2.72	0.95
NM_012880	Sod3	Superoxide dismutase 3, extracellular	2.38	0.73	2.51	0.58	2.36	1.05	2.64	1.00
NM_053576	Prdx6	Peroxiredoxin 6	2.21	0.66	2.64	0.83	2.65	0.99	2.93	0.83
NM_012837	Cst3	Cystatin C	2.06	0.52	2.18	0.63	2.07	0.62	2.08	0.63
XM_214236	Nudt15	Nudix (nucleoside diphosphate linked moiety X)-type 15	1.90	0.59	1.57	0.53	1.51	0.49	1.55	0.48
NM_017051	Sod2	Superoxide dismutase 2, mitochondrial	1.70	0.47	1.87	0.59	1.32	0.43	1.62	0.51
NM_017305	Gclm	Glutamate cysteine ligase, modifier subunit	1.69	0.44	1.31	0.43	1.32	0.42	1.08	0.42
NM_012815	Gclc	Glutamate-cysteine ligase, catalytic subunit	1.67	0.49	1.14	0.32	1.23	0.33	−1.04	0.47
NM_057143	Park7	Fertility protein SP22	1.56	0.43	1.68	0.45	1.52	0.45	1.53	0.56
NM_012962	Gss	Glutathione synthetase	1.48	0.42	1.66	0.52	1.61	0.46	1.22	0.38
NM_030826	Gpx1	Glutathione peroxidase 1	1.48	0.36	1.67	0.42	1.42	0.37	1.53	0.57
NM_019354	Ucp2	Uncoupling protein 2	1.47	0.43	1.60	0.47	1.17	0.56	2.34	0.70
NM_031614	Txnrd1	Thioredoxin reductase 1	1.46	0.47	−1.15	0.23	−1.13	0.28	−1.60	0.18
XM_216452	Dhcr24	24-Dehydrocholesterol reductase (predicted)	1.20	0.36	−1.41	0.27	−1.05	0.65	−1.66	0.31
XM_579339	Serpine1	Serine (or cysteine) Proteinase inhibitor, clade E, member 1	−1.10	0.31	−1.69	0.20	−1.67	0.31	−2.11	0.13
NM_017365	elfin,Pdlim1	PDZ and LIM domain 1	−1.18	0.26	−1.31	0.21	−1.62	0.21	−1.46	0.20
NM_017258	Btg1	B-cell translocation gene 1, anti-proliferative	−1.33	0.25	−1.32	0.22	−1.27	0.27	−1.54	0.28
NM_031056	Mmp14	Matrix metalloproteinase 14 (membrane-inserted)	−1.42	0.20	−1.71	0.16	−2.04	0.14	−2.01	0.13
NM_053769	Dusp1	Dual specificity phosphatase 1	−1.54	0.32	−2.61	0.18	−1.73	0.36	−2.61	0.24
XM_216403	Xpa	Xeroderma pigmentosum, complementation group A	−1.55	0.18	−1.44	0.22	−1.57	0.20	−1.55	0.18
NM_017025	Ldha	Lactate dehydrogenase A	−1.55	0.18	−2.35	0.12	−2.20	0.12	−2.45	0.12
NM_024134	Ddit3	DNA-damage inducible transcript 3	−2.00	0.15	−2.41	0.12	−2.38	0.12	−2.74	0.11
NM_001008767	Txnip	Up-regulated by 1,25-dihydroxyvitamin D-3	−3.59	0.22	−2.32	0.11	−4.98	0.22	−1.97	0.15
NM_019292	Ca3	Carbonic anhydrase 3	−9.36	0.06	−5.14	0.05	−12.0	0.13	−6.89	0.08
XM_213440	Col1a1	Collagen, type 1, α1	−16.8	0.02	−8.92	0.03	−19.1	0.04	−19.8	0.02

Continued

Table 1 Continued

GenBank	Symbols	Gene name	Time							
			8 hrs	S.E. (±)	15 hrs	S.E. (±)	24 hrs	S.E. (±)	48 hrs	S.E. (±)
Response to unfolded protein										
NM_053612	Hspb8	Heat shock 22 kD protein 8	3.64	0.89	2.98	0.67	2.91	0.72	2.81	0.83
XM_215549	OSP94	Osmotic stress protein 94 kD (predicted)	3.55	1.23	3.21	0.97	3.00	0.78	2.98	1.53
NM_138887	Hspb6	Heat shock protein, α-crystallin-related, B6	1.98	0.58	2.25	0.69	1.89	0.69	2.03	0.92
NM_175761	Hspca	HEAT shock protein 1, α	1.81	0.48	1.80	0.60	1.61	0.57	1.42	0.78
XM_579648	Ero1l	Rattus norvegicus ERO1-like	−1.40	0.20	−1.53	0.20	−1.51	0.20	−1.59	0.19
NM_031789	Nfe2l2	Nuclear factor, erythroid derived 2, like 2	−1.53	0.21	−1.79	0.16	−1.88	0.15	−1.72	0.20
NM_053523	Herpud1	Homocysteine-inducible, endoplasmic reticulum stress-inducible, ubiquitin-like domain member 1	−1.64	0.17	−1.57	0.18	−1.77	0.18	−1.64	0.24
XM_579186	Txndc4	Thioredoxin domain containing 4 (endoplasmic reticulum)	−1.65	0.18	−1.56	0.18	−1.79	0.17	−1.78	0.22
NM_022232	Dnajc3	Protein kinase inhibitor p58	−1.75	0.18	−1.78	0.18	−1.94	0.17	−1.99	0.21
NM_001004210	Xbp1	X-box binding protein 1	−2.09	0.15	−2.32	0.12	−2.49	0.11	−2.61	0.11
NM_001005562	Creb3l1	cAMP responsive element binding protein 3-like 1	−7.08	0.04	−6.23	0.05	−7.43	0.04	−7.65	0.04
Calcium ion homeostasis										
NM_017333	Ednrb	Endothelin receptor type B	4.64	1.30	4.72	1.49	4.41	1.46	4.94	1.35
NM_013179	Hcrt	Hypocretin	3.07	2.31	3.31	1.04	2.64	1.93	4.51	1.27
NM_017338	Calca	Calcitonin/calcitonin-related polypeptide, ·	1.93	0.65	2.11	0.62	1.85	0.57	1.99	0.68
XM_341418	Edg4	Endothelial differentiation, lysophosphatidic acid G-protein-coupled receptor 4 (predicted)	1.90	0.58	2.50	0.77	2.04	0.66	1.96	1.07
NM_031648	Fxyd1	FXYD domain-containing ion transport regulator 1	1.83	0.70	2.46	0.81	1.88	0.80	2.88	1.20
XM_579178	S100a1	S100 calcium binding protein A1	1.74	0.79	2.04	0.62	1.86	0.85	2.38	0.85
NM_012713	Prkcb1	Protein kinase C, β1	1.59	0.80	−1.14	0.55	1.27	0.82	−1.24	0.68
NM_017010	Grin1	Glutamate receptor, ionotropic, N-methyl D-aspartate 1	1.56	0.84	−1.47	0.70	1.16	1.31	−1.71	0.63
NM_016991	Adra1b	Adrenergic receptor, α1b	−1.24	0.24	−1.57	0.19	−1.44	0.22	−1.72	0.16
NM_001007235	Itpr1	Inositol 1,4,5-triphosphate receptor 1	−1.31	0.31	−1.54	0.31	−1.44	0.31	−1.93	0.33
NM_138535.1	Grip2	Glutamate receptor interacting protein 2	−1.39	0.21	−1.59	0.17	−1.13	0.27	−1.81	0.18
NM_030987	Gnb1	Guanine nucleotide binding protein, β1	−1.42	0.21	−1.88	0.18	−1.64	0.20	−1.92	0.22
NM_053867	Tpt1	Tumour protein, translationally-controlled 1	−1.43	0.23	−1.53	0.21	−1.42	0.21	−1.61	0.18
NM_021666	Trdn	Triadin	−1.57	0.17	−1.58	0.19	−1.52	0.18	−1.55	0.18
NM_031123	Stc1	Stanniocalcin 1	−1.62	0.37	−1.84	0.19	−1.49	0.24	−2.10	0.25
NM_021663	Nucb2	Nucleobindin 2	−1.69	0.18	−1.67	0.21	−1.75	0.18	−1.82	0.33
NM_023970	Trpv4	Transient receptor potential cation channel, subfamily V, member 4	−1.71	0.16	−1.44	0.25	−1.72	0.17	−1.62	0.14
NM_017022	Itgb1	Integrin β1 (fibronectin receptor β)	−1.77	0.18	−1.87	0.21	−2.15	0.14	−2.42	0.23
NM_012714	Gipr	Gastric inhibitory polypeptide receptor	−2.23	0.14	−3.09	0.10	−2.34	0.18	−3.46	0.08
NM_053936	Edg2	Endothelial differentiation, lysophosphatidic acid G-protein--coupled receptor, 2	−3.13	0.28	−2.26	0.23	−3.85	0.17	−2.17	0.14
XM_579462	Pln	Phospholamban	−7.16	0.04	−6.34	0.05	−6.56	0.05	−6.18	0.04
NM_053019	Avpr1a	Arginine vasopressin receptor 1A	−10.1	0.03	−9.82	0.03	−9.53	0.03	−10.9	0.03

Continued

Table 1 Continued

GenBank	Symbols	Gene name	Time 8 hrs	S.E. (±)	15 hrs	S.E. (±)	24 hrs	S.E. (±)	48 hrs	S.E. (±)
Vesicle transport										
NM_053555.1	Vamp5	Vesicle-associated membrane protein 5	1.65	0.52	2.02	0.71	1.35	0.50	1.98	0.59
NM_057097.1	Vamp3	Vesicle-associated membrane protein 3	1.55	0.38	1.69	0.40	1.47	0.45	1.48	0.60
NM_138835.1	Syt12	Synaptotagmin 12	1.56	0.46	1.15	0.35	1.27	0.35	1.17	0.33
XM_343205.2	Syt1	Synaptotagmin 1	1.33	1.08	−2.13	0.90	1.09	1.59	−1.96	0.85
Inflammatory response										
NM_133624.1	Gbp2	Guanylate nucleotide binding protein 2	17.5	7.13	20.0	6.93	14.0	3.77	12.9	4.69
NM_212466	Bf	B-factor, properdin	6.47	3.81	9.28	9.00	7.12	1.98	10.9	4.90
NM_172222	C2	Complement component 2	3.55	0.97	4.03	1.22	3.17	0.90	4.50	1.51
XM_215095.3	Gprc5b	G protein-coupled receptor, family C, group 5, member B	3.07	1.03	2.75	0.78	2.29	0.69	3.32	1.43
NM_199093	Serping1	Serine (or cysteine) peptidase inhibitor, clade G, member 1	2.80	2.06	2.48	1.23	2.40	1.15	3.67	2.05
NM_012488	A2m	·2-Macroglobulin	2.61	0.64	3.49	0.82	2.60	1.26	3.76	1.10
NM_019363	Axo1	Aldehyde oxidase 1	2.53	0.70	5.69	3.33	4.03	2.37	2.83	0.84
XM_573457.1	Gpr37l1	G protein-coupled receptor 37-like 1 (predicted)	2.52	0.85	3.05	0.98	2.63	0.88	3.62	1.94
NM_138502	Mgll	Monoglyceride lipase	2.51	1.08	2.16	0.81	2.21	0.79	2.31	0.72
NM_152242.1	Gpr56	G protein-coupled receptor 56	2.42	0.73	2.16	0.53	2.23	0.64	2.10	0.68
NM_212541	Ng22	Ng22 protein	1.94	0.64	2.16	0.68	1.66	0.51	2.12	0.65
NM_138900	C1s	Complement component 1, s subcomponent	1.91	0.54	2.18	0.82	1.75	0.51	1.92	0.70
NM_031351	Atrn	Attractin	1.89	0.52	1.68	0.52	1.84	0.53	1.42	0.43
NM_031007.1	Adcy2	Adenylate cyclase 2	1.88	0.51	1.78	0.55	1.80	0.52	1.78	0.56
XM_579383.1	Adcyap1	Adenylate cyclase activating polypeptide 1 (predicted)	1.74	1.96	−1.90	0.30	1.14	2.35	−2.01	0.25
NM_013157	Ass	Argininosuccinate synthetase	1.71	2.33	1.05	0.36	1.52	1.49	−1.05	0.30
NM_031634	Mefv	MEDITERRANEAN fever	1.61	0.47	1.77	0.48	1.73	0.62	1.97	0.56
NM_021690.1	Rapgef3	cAMP-regulated guanine nucleotide exchange factor I	1.58	0.40	1.78	0.48	1.71	0.52	1.77	0.48
XM_579359	Cd59	CD59 antigen	1.40	0.45	1.47	0.39	1.23	0.79	2.00	0.56
NM_053734	Ncf1	Neutrophil cytosolic factor 1	1.32	0.42	1.18	0.44	1.36	0.74	2.06	1.32
NM_212490	Atp6v1g2	ATPase, H+ transporting, V1 subunit G isoform 2	1.31	0.75	−1.50	0.62	1.18	0.88	−1.50	0.78
NM_022216.1	Gpr20	G protein-coupled receptor 20	1.25	0.37	1.70	0.56	1.34	0.44	1.64	0.46
NM_153318	Cyp4f6	Cytochrome P450 4F6	1.21	0.30	1.51	0.39	1.25	0.37	1.42	0.41
NM_001009353	Pla2g7	Phospholipase A2, group VII (platelet-activating factor acetylhydrolase, plasma)	1.20	0.43	1.24	0.41	1.27	0.78	1.74	1.25
NM_024157	Cfi	Complement factor I	1.19	0.33	1.20	0.33	1.20	0.34	1.59	0.50
NM_022236.1	Pde10a	Phosphodiesterase 10A	1.08	0.30	−1.52	0.38	−1.30	0.29	−1.70	0.36
XM_579389	Tf	Transferrin	−1.05	1.91	−1.50	0.82	−1.04	0.76	2.02	6.19

Continued

Table 1 Continued

GenBank	Symbols	Gene name	Time							
			8 hrs	S.E. (±)	15 hrs	S.E. (±)	24 hrs	S.E. (±)	48 hrs	S.E. (±)
NM_017196	Aif1	Allograft inflammatory factor 1	−1.15	0.56	−1.29	0.92	−1.11	1.11	1.79	1.40
NM_024125	Cebpb	CCAAT/enhancer binding protein (C/EBP), β	−1.25	0.21	−1.55	0.21	−1.27	0.22	−1.53	0.21
XM_342092	Vars2	Valyl-tRNA synthetase 2	−1.31	0.21	−1.56	0.19	−1.38	0.19	−2.08	0.14
NM_052809	Cdo1	Cysteine dioxygenase 1, cytosolic	−1.34	0.23	−1.99	0.15	−1.81	0.16	−1.62	0.17
NM_024486	Acvr1	Activin A receptor, type 1	−1.38	0.23	−1.46	0.21	−1.65	0.19	−1.61	0.17
NM_012666	Tac1	Tachykinin 1	−1.50	0.23	−2.32	0.14	−1.60	0.34	−2.47	0.13
XM_239239	Map2k3	Mitogen-activated protein kinase kinase 3 (predicted)	−1.67	0.18	−2.12	0.14	−2.08	0.15	−2.46	0.15
NM_130409	Cfh	Complement component factor H	−1.68	0.18	−1.25	0.25	−1.57	0.19	1.02	0.32
XM_579400	Lbp	Lipopolysaccharide binding protein	−1.81	0.19	−1.39	0.23	−1.63	0.21	−1.09	0.44
XM_343169	And	Adipsin	−2.07	0.14	−2.14	0.15	−1.83	0.15	−1.88	0.14
NM_019143	Fn1	Fibronectin 1	−2.22	0.17	−2.15	0.20	−2.43	0.11	−3.73	0.22
NM_019262	C1qb	Complement component 1, q subcomponent, β polypeptide	−2.42	0.22	−2.81	0.29	−2.08	0.71	−1.38	0.54
NM_001008524	C1qg	Complement component 1, q subcomponent, gamma polypeptide	−2.49	0.15	−2.97	0.18	−2.17	0.39	−1.44	0.47
NM_017232	Ptgs2	Prostaglandin-endoperoxide synthase 2	−3.59	0.16	−6.51	0.06	−3.84	0.13	−6.18	0.08
XM_240184	Nfatc4	Nuclear factor of activated T cells, cytoplasmic, calcineurin-dependent 4 (predicted)	−15.4	0.06	−8.20	0.06	−14.8	0.04	−10.4	0.03
Chemotaxis										
NM_031530	Ccl2	Chemokine (C-C motif) ligand 2	6.01	8.84	2.87	2.48	3.68	9.35	2.66	2.08
NM_182952.2	Cxcl11	Chemokine (C-X-C motif) ligand 11	5.24	1.72	6.02	8.94	2.80	0.81	2.34	1.31
NM_022205	Cxcr4	Chemokine (C-X-C motif) receptor 4	3.14	1.20	4.19	1.11	2.81	0.82	3.56	2.11
NM_012953	Fosl1	Fos-like antigen 1	2.97	1.17	−1.04	0.27	1.47	1.19	1.02	0.25
NM_001007612	Ccl7	Chemokine (C-C motif) ligand 7	2.80	3.76	2.09	1.76	2.01	3.77	1.56	0.75
NM_139089	Cxcl10	Chemokine (C-X-C motif) ligand 10	2.67	1.43	10.3	23.6	3.87	2.87	3.86	3.14
NM_053953.1	Il1r2	Interleukin 1 receptor, type II	2.42	1.05	2.23	0.71	2.28	0.68	1.87	0.85
NM_145672	Cxcl9	Chemokine (C-X-C motif) ligand 9	2.13	1.58	3.09	2.97	2.42	0.75	1.94	1.24
NM_012747.2	Stat3	Signal transducer and activator of transcription 3	2.0	0.5	1.57	0.38	1.64	0.46	1.45	0.38
NM_030845	Cxcl1	Chemokine (C-X-C motif) ligand 1	1.96	4.51	−1.30	0.32	1.64	4.95	1.18	1.07
XM_234422.3	c-fos	c-Fos oncogene	1.8	0.5	1.61	0.45	1.52	0.52	1.54	0.51
NM_134455	Cx3cl1	Chemokine (C-X3-C motif) ligand 1	1.58	0.62	1.01	0.46	1.32	0.88	−1.22	0.74

Continued

Table 1 Continued

GenBank	Symbols	Gene name	Time							
			8 hrs	S.E. (±)	15 hrs	S.E. (±)	24 hrs	S.E. (±)	48 hrs	S.E. (±)
NM_031512.1	Il1b	Interleukin 1β	1.57	0.77	1.30	0.48	1.30	0.42	1.46	0.62
NM_017020.1	Il6r	Interleukin 6 receptor	1.54	0.44	1.21	0.36	1.28	0.37	1.28	0.33
NM_031116	Ccl5	Chemokine (C-C motif) ligand 5	1.43	0.40	2.96	2.76	1.80	0.48	3.03	2.40
NM_139111	Cklf1	Chemokine-like factor 1	1.24	0.38	1.39	0.44	1.13	0.31	1.89	0.56
NM_031643	Map2k1	Mitogen-activated protein kinase kinase 1	1.08	0.30	−1.27	0.29	−1.14	0.22	−1.55	0.49
XM_342823	Ccl27	Chemokine (C-C motif) ligand 27 (predicted)	−1.12	0.28	−1.55	0.25	−1.16	0.38	−1.62	0.19
XM_579590	Enpp2	Ectonucleotide pyrophosphatase/phosphodiesterase 2	−1.61	0.29	−1.22	0.26	−1.80	0.21	−1.59	0.18
NM_031327	Cyr61	Cysteine rich protein 61	−1.65	0.24	−2.00	0.19	−1.90	0.26	−2.22	0.25
NM_031836	Vegfa	Vascular endothelial growth factor A	−1.69	0.16	−1.79	0.14	−1.78	0.16	−1.87	0.15
NM_022177	Cxcl12	Chemokine (C-X-C motif) ligand 12	−1.81	0.18	−1.71	0.17	−1.70	0.17	−1.16	0.29
NM_001007729	Pf4	Platelet factor 4	−1.92	0.33	−2.98	0.10	−1.95	0.23	−2.36	0.12
NM_012881	Spp1	Secreted phosphoprotein 1	−3.05	0.19	−1.86	0.29	−3.08	0.10	−1.40	0.64
NM_019233	Ccl20	Chemokine (C-C motif) ligand 20	−3.09	0.44	−2.17	0.41	−1.94	0.94	−2.62	0.30

Genes with a minimum fold change of ±1.5 for at least one out of the four time points passed one-way ANOVA analysis and are significant with $P < 0.05$. Data are expressed as fold-change ± S.E. Blue = genes that were up-regulated. Red = genes that were down-regulated.

scriptional and translational factors. The significance of changes in expression of these cell cycle genes in the absence of visible cell death upon axotomy is intriguing as there is increasing evidence showing that cell cycle proteins do play novel, alternate neuronal functions [19].

Ion homeostasis response genes

Disruption to ion balance after axotomy was reflected in the varied expression of genes that control ion entry channels such as *Fxyd1*, *Adra1b*, *Edg2*, *Itpr1*, *Trpv4* and *Avpr1a*. In particular, we noticed an elevated gene expression of calcium-activated proteins such as *Capn3* and *S100A1* that play pivotal roles in cell death, axonal resealing and cytoskeleton remodelling. Temporal expression of calcium-associated members such as *Camk2b*, *PKC* and *Grin1* further demonstrated a likely link between calcium levels and neurorepair. Furthermore, elevated gene expression of calcium-activated *AMPK*, a key regulator of energy balance, and its upstream activators namely *Cntf* and interleukins might signify a mechanism in place to compensate energy deficits during ion and/or metabolites imbalance states.

Inflammatory response genes

Inflammation is part of a complex 'double-edged sword' response to injury that facilitates healing and/or elicits death. Quite interestingly, the presence of inflammation-causing genes such as *Bf*, *C2*, *Atrn* and *Ncf1* was accompanied by an increased expression of cAMP regulatory genes namely *Adcy*, *Adcyap*, *Gpr* and *Rapgef*. Interplay of various chemokines and cytokines was evident from the gene regulation profiles of numerous chemokine ligands (*Ccl* and *Cxcl* families), cytokine (*Il1b*), and their receptors (*Cxcr*, *Il1r2* and *Il6r*). Cytokine-activated transcription factors such as *Stat3* and *c-fos* that drive cell proliferation, signal transduction and cytoskeleton restructuring were also increased.

Validation of microarray analysis

Microarray data for all time points after axonal injury were validated by RT-PCR against selected genes as presented in Table 2. The trend of gene expression changes for each selected target obtained from RT-PCR was similar to its microarray data. In gen-

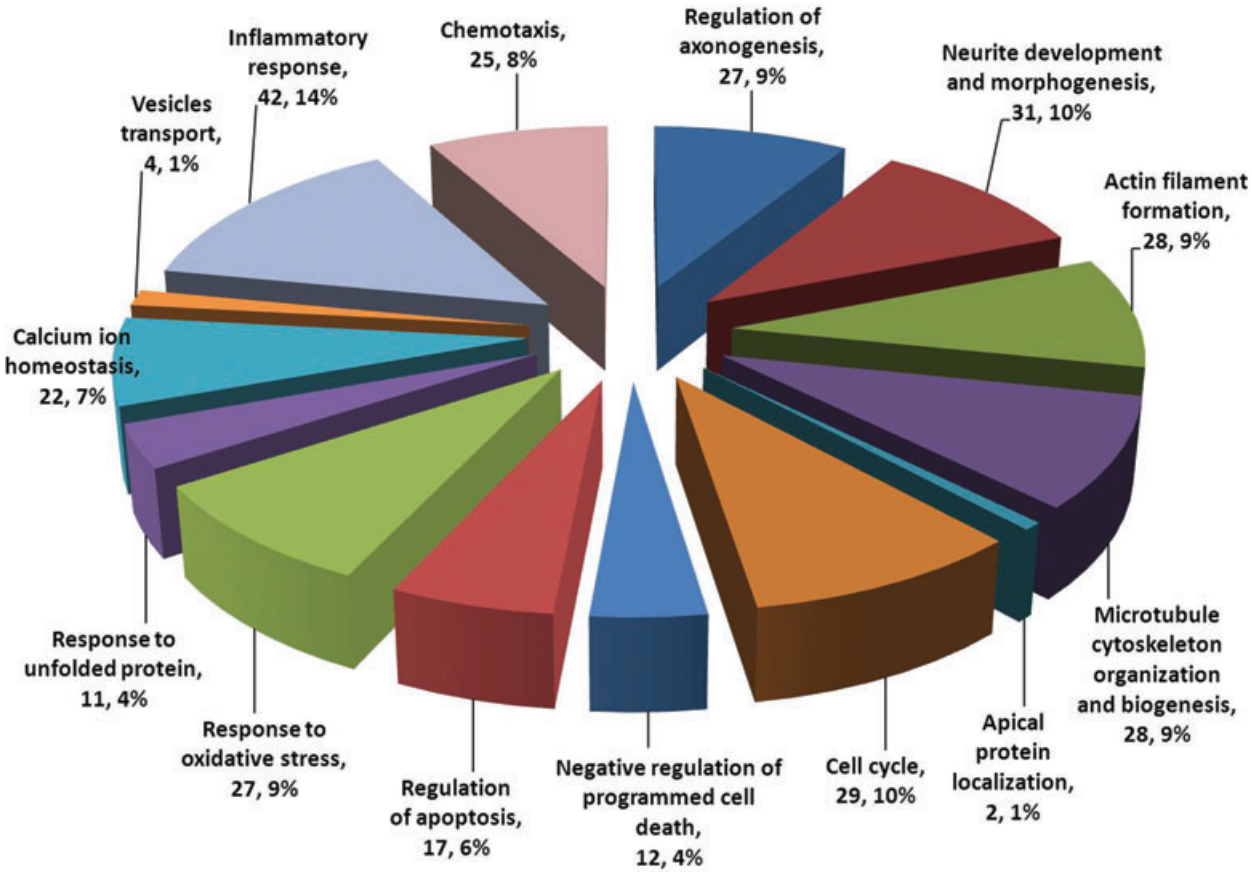

Fig. 1 Pie chart annotating number and percentage of genes identified in each of the 14 biological processes. A total of 305 statistically significant regulated genes were identified by DAVID. Each gene was classified into one of its most relevant biological processes categorized according to Gene Ontology to avoid overestimation.

eral, this confirmed the reliability of the gene expression profiles attained.

Discussion

Severance of fasciculated axonal bundles in mature rat neuronal clusters in culture has been used previously to study and characterize the cytoskeletal dynamics of regenerative sprouting after axonal injury [6]. Using the same *in vitro* model, we have applied a DNA microarray approach to gain mechanistic insight into the key molecular determinates that underlie neurite regeneration after axotomy at a transcriptomic level. Briefly, we found that regenerative sprouting is a complicated process that involves complex cytoskeleton dynamics and vigilant control of secondary processes such as oxidative stress, ion homeostasis and inflammation. These secondary processes have to be tightly regulated to ensure neurite regeneration without causing evident cell death. Physiologically, diffuse axonal injury is one of the many key pathological features associated with head trauma. Upon trauma, stretched axons become brittle and tear. This situation is immediately salvaged by the damaged neurons' intrinsic capacity to regenerate. However, mechanisms are activated for cell demise when the injury is beyond redemption. Through transcriptomic studies, we may identify crucial cellular pathways that facilitate regeneration and manipulate them whenever necessary to lessen damage and avoid irreversible apoptosis.

Neurite cytoskeleton reorganization

In accordance with the study by Chuckowree and Vickers [6], we confirmed that adaptive sprouting of neurons after injury involves substantial cytoskeleton reorganization. For an axon to regenerate, its neurite arm, which is predominately composed of microtubules,

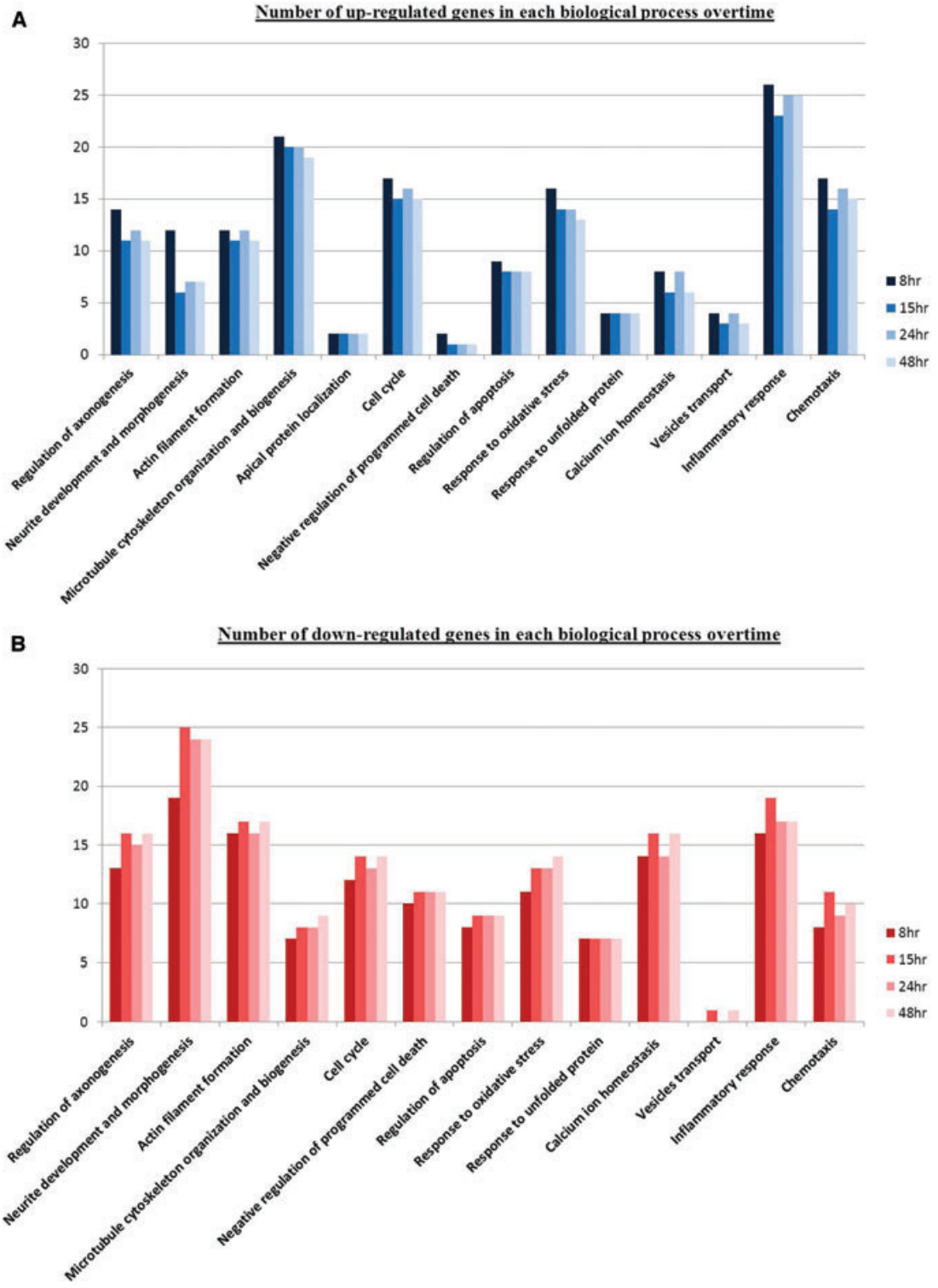

Fig. 2 Comparison of biological processes associated with axotomized neurons across 8, 15, 24 and 48 hrs post-injury. Bar chart shows the distribution of up-regulated (**A**) and down-regulated (**B**) genes. Differentially transcribed genes involved in the number count were statistically significant. Overall, the genomic profiles for particular biological processes at 8 hrs were slightly distinct as compared to the other time points.

Table 2 Validation of microarray data using real-time PCR technique on rat neuronal samples, 8, 15, 24 and 48 hrs after axotomy

Gene title	Symbol	8 hrs		15 hrs		24 hrs		48 hrs	
		Microarray	Real-time PCR	Microarray	Real-time PCR	Microarray	Real-time PCR	Microarray	Real-time PCR
Neural Wiskott–Aldrich syndrome protein	N-WASP	3.7 ± 1.3	7.4 ± 2.4	4.8 ± 1.6	2.7 ± 0.5	3.5 ± 2.1	1.7 ± 0.4	4.2 ± 2.4	2.9 ± 0.3
Chemokine (C-X-C motif) ligand 10	Cxcl10	2.7 ± 1.4	2.5 ± 0.8	10.3 ± 23.6	11.1 ± 3.3	3.9 ± 2.9	3.9 ± 2.5	3.9 ± 3.1	2.6 ± 0.8
Dynein, cytoplasmic, light chain 2B (predicted)	Dncl2b	20.8 ± 6.6	9.3 ± 2.3	23.9 ± 7.2	10.4 ± 3.5	16.4 ± 13.5	10.4 ± 3.9	22.5 ± 10.6	10.0 ± 1.7
Guanylate nucleotide binding protein 2	Gbp2	17.5 ± 7.1	7.8 ± 3.6	20.0 ± 6.9	9.2 ± 2.8	14.0 ± 3.8	11.4 ± 5.0	12.9 ± 4.7	9.9 ± 2.9
Chemokine (C-X-C motif) ligand 11	Cxcl11	5.2 ± 1.7	3.2 ± 1.1	6.0 ± 8.9	4.8 ± 1.7	2.8 ± 0.8	4.8 ± 1.3	2.3 ± 1.3	4.0 ± 1.1
Aurora kinase B	Aurkb	5.0 ± 2.0	3.7 ± 1.0	5.9 ± 1.7	5.4 ± 1.3	4.0 ± 1.6	5.0 ± 1.2	5.8 ± 1.7	4.8 ± 1.6

Data are expressed as fold-change ± S.E.

needs to be extended accordingly. This involves microtubule formation and stabilization. Tubulins are fundamental for microtubule formation and this could explain their augmented gene expression. Stabilizing these newly formed microtubules is pivotal and this entails a concerted regulation of various microtubule destabilizing and stabilizing proteins. Elevated gene expression of *Notch1*, alongside decreased expression of *Stmn*, *Cspg2* and *Spg4*, is consistent with this process. It has been found that microtubule stabilization could promote axon regeneration by preventing chondroitin sulphate proteoglycan (*Cspg*) accumulation at lesion site [20]. This stabilization could be mediated by *Notch* activation whereby it down-regulated spastin (*Spg*) expression, a microtubule severing protein, and deterred axonal degeneration in primary cortical neurons [21]. Stamins (*Stmn*) in general destabilize microtubules by preventing their assembly and promoting their disassembly.

The regenerating growth cone acts such as a molecular conveyor belt whereby actin bundles at the proximal end are constantly fragmented by actin-destabilizing or severing proteins. Released actin fragments are then retrogradely transported and reassembled at the leading edge with help from nucleation-promoting factors [22]. These changes were reflected by the down-regulated gene expression of actin regulators namely *Pfn*, *Cdc42*, *Arp2/3* [23, 24]. In contrast, *NWASP* and *Gas7* gene expression were up-regulated by an average of 3- and 1.5-fold, respectively, throughout [25, 26]. As such, it is imperative to account for the contrasting regulation of *NWASP*, *Arp2/3* and *Cdc42*. *NWASP* and *Arp2/3* are undeniably the master components of actin polymerization. During neurite regrowth, actin dynamics unlike microtubules steer towards instability, a phenomenon observed due to the complex processes governing polymerization and depolymerization of actin filament to support growth cone steering. Interestingly, Erin D.G and Matthew D.W critically reviewed that the way *Arp2/3* affects actin polymerization is more dependent on its activity regulated by ATP rather than its expression [27]. It was mentioned that binding of *WASP* to ATP bound *Arp2/3* and G actin, primes the complex and creates a nucleation point for daughter filaments formation. Subsequent ATP hydrolysis on *Arp2* after nucleation has been temporally and functionally linked to actin branch disassembly. The authors also brought up the importance of recycling *Arp2/3* itself for the formation of new actin processes, an event closely associated with actin recycling. With that, the possibility of regulating already expressed *Arp2/3* proteins by ATP in neurons and the fact that it can be recycled could potentially explain the redundant need for its expression after axotomy. Unlike *Arp2/3*, *NWASP* is not directly regulated by ATP binding but its relevance is to elicit an active conformation of *Arp2/3* for nucleation by physically binding to it. As such, our data illuminate an interesting questionnaire on how *NWASP* is being regulated in regards to neurite regeneration. Moreover, apart from *NWASP* physical interaction with *Arp2/3* to direct actin polymerization, it also serves as focal points where transduced signals converge to orchestrate actin polymerization dynamics [28]. Hence, *NWASP* importance in connecting multiple signalling pathways to initiate actin assembly as well as how it is regulated could possibly account for its elevated expression in comparison to *Arp2/3*. As for *Cdc42*, unlike *NWASP* and *Arp2/3*, there has been evidence showing that *NWASP* recruitment of *Arp2/3* that results in the formation of membrane protrusions and processes could occur *via* a *Cdc42*-independent manner, at least for neurite outgrowth of hippocampal neurons [26]. Because of the way actin proteins are recycled in the growth cone, this further explains the redundant need for newly synthesized actins and they were generally down-regulated transcriptionally following axonal injury. Recycling is essential to prevent excessive actin build-up that could thwart neuronal advances. This assumption is further supported by the

heightened expression of myosin genes, which encode motor molecules that transport actins in a retrograde fashion. Using fluorescent speckle microscopy, it was found that inhibition of myosin II not only perturbed actin retrograde flow and affected neuronal growth but its contraction forces were also required to recycle actin fragments for growth cone formation [29]. Together, our gene profiling data showed that neurite regeneration is an event that involves stabilization of microtubules and dynamic instability of actin filaments [7].

Further evidence of the dynamic response of the cytoskeleton to axotomy was the elevated expression of *Tekt 1* and *2*. These represent a group of cilia microtubule structural proteins, and supports an unexpected discovery that neuronal cilia might be vital for modulating signalling pathways to coordinate neuronal processes such as axonal guidance [30]. This highlights the need for further investigation on the roles of cilia-associated proteins in neurobiological events such as axotomy.

The importance of protein trafficking in axonal regeneration was indicated by the varied gene expression of motor proteins involved in cytoskeletal transport such as *Dnc*, *Dna*, *Kif*, *Myh*, *Tpm* and machinery factors linked to membrane vesicles such as *Syt*, *Vamp*, *Stx*. This clearly illustrated retrograde transport of injury signals from cut site to cell body which then evoked membrane expansion processes that involve cargo trafficking of cytoskeletal proteins and even neurotropic factors to promote axonal regrowth. Dynein-derived forces in particular, are able to oppose axon retraction and permit microtubules to advance [31].

Moreover, neurite regeneration is a process that involves reciprocal regulation of permissive and repulsive axon guidance cues. Neurotrophic factors, for instance, are capable of directing axonal regrowth in damaged neurons. *Bdnf* can sustain axon regeneration upon various nerve and brain injuries [32, 33] and overexpression of its receptor *NtrkB* was also found to elicit corticospinal axonal regeneration [34]. Here, transient gene expression of *Bdnf* and *Ntrks* at 8 hrs could highlight the probable importance of these molecules in the recovery process during the initial phase but not as much after specific projections had been formed. Most repulsive guidance molecules on the other hand, inhibit and deter axonal regrowth after injury. *Sema3a* is one such example. Chemically inhibiting *Sema3a* prevented its binding to neuropilin and enhanced neural regeneration in damage axons [35]. *Eph/Ephrin* signalling which controls axon guidance by contact repulsion also inhibits regeneration of axons following injury in neurons [36]. Similarly, our transcriptomic data concurred that these molecules and their receptors mainly *Efn*, *Sema*, *Slit*, *Bmp*, *Nrp*, *Plxd* and *Eph* were not favoured during neurite regrowth.

Notably, some neurite promoting factors including *Apoe*, *Cntf* and *Lama5* were also significantly up-regulated. *Apoe* is required for lipid delivery for axon regrowth upon nerve crush injury [37] whereas *Lama* serves as a crucial extracellular matrix adhesion molecule along which axons would grow and thus permit regeneration in central neurons [38, 39]. Although *Cntf* is found mainly in astrocytes, it is also expressed in cortical neurons [40]. Being a cytokine-induced neurotrophic factor, it can potentiate axon regeneration in optic and spinal nerve injuries [41–43]. Overall, our results demonstrate that to facilitate axonal regrowth, the injured neurons themselves adapt to ensure that the cellular environment is permissive to regeneration *via* temporal generation of positive cues, concomitant restriction of negative cues and expression of neurotrophic factors.

Apart from the genes that regulate neurite cytoskeleton, our data have further shown that various genes commonly linked to secondary processes such as oxidative stress, apoptosis, cell cycle, calcium homeostasis and inflammation are also important in dictating the regenerative process of axonally cut neurons and their possible roles are briefly discussed as follow.

Oxidative stress

Reactive oxygen species (ROS) are inevitable harmful by-products of cellular activities. Oxidative stress, which could result in cell death, ensues when the build-up of ROS in cells overwhelm existing biological antioxidants under normal conditions. This occurs in neurons after axonal injury. To counteract such insult, our study showed that genes responsible for GSH synthesis and various antioxidant enzymes (*Sods*, *Prdxs*, *Gpx*) were elevated to alleviate the stress. This demonstrated that neurons have the transcriptional capability to activate these vital mechanisms for their fight against oxidative insult to prevent death and assist in regenerative sprouting.

Several heat shock proteins (*Hsp*) were also transcriptionally up-regulated. Mainly, *Hsp* act as molecular chaperones to refold misfolded proteins and prevent deleterious protein build-up. Intriguingly, small *Hsp* (12–43 kD) are viewed as vital neuroprotectants in several neurological disorders [44]. *Hsp27* whose gene expression was up-regulated by $\geq$4-folds post-injury could suppress cytochrome *c*–mediated cell death [45]. Besides, it could interact, modulate and remodel neuronal cytoskeleton [46, 47]. As such, in addition to its protein refolding function, local gene expression of *Hsp* after axotomy might serve as anti-apoptotic and neurite regrowth signals.

Programmed cell death (PCD)

PCD is a process regulated by proto-oncogenes. It is logical that for an injured neuron to successfully regenerate, it must avoid axotomy-induced cell death. It is possible that apoptotic genes such as *Apaf1*, *Bnips*, *Casp3*, *11* and *12* were down-regulated in our study as an intrinsic protective mechanism to facilitate regeneration. This is supported by the fact that axotomized neuronal clusters *in vitro* did not result in evident cell death [6]. Similarly, studies have shown that overexpression of anti-apoptotic proteins could save neurons from axotomy-induced cell death [48, 49]. However, it is important to note that stringent control of apoptotic genes expression in denial of cell death in this case does not necessarily assist or speed up neurite regeneration, and probably indicates that neuron survival and neurite regeneration represent two distinct, although closely linked, processes within axotomized neurons.

Cell cycle

Cell cycle activation in response to DNA damage during extreme cellular stress could lead to the demise of neurons [50]. Interestingly, several cell cycle proteins were recently found to possess distinct, alternate neuronal functions that are independent from their cell cycle roles [19]. Plausibly, this mirrors our case of neurite regeneration in which certain cell cycle genes were elevated despite the down-regulation of several apoptotic genes consistent with cell death not being prominent. *Aurkb*, for example is a cell cycle kinase that remodels microtubule arrays for precise cell division [51, 52]. Its elevated gene expression could possibly reflect a function in neurite regrowth, a process akin to its involvement in cell division, because both processes involve complex cytoskeleton reorganization. However, functional biological studies are required to ascertain this speculation. Intriguingly, Aurora A kinase (*Aurka*), a sister kinase of *Aurkb* that is also known for its mitotic roles, had lately been reported by two separate groups to play a crucial role in the establishment of neuronal polarity [53, 54].

A more specific example involves *Klf4*, which was significantly down-regulated in our studies. Early studies show that *Klf4* is a key cell cycle checkpoint transcription factor and it causes G_1/S arrest by activating genes that are potent inhibitors of proliferation [55]. Recently, an alternate neuronal function of *Klf4* was discovered whereby its overexpression in cortical neurons impeded neurite outgrowth while its knockout in retinal ganglion cells (RGCs) increased axon regeneration after crush injury [56]. Hence, beside cell cycle re-entry causing neuronal death, diverse gene expression of cell cycle proteins after axotomy could also signify alternate and unexpected functions for these proteins to regulate the cytoskeleton and promote axonal regeneration.

Calcium homeostasis

Calcium homeostasis after axotomy is vital as it determines survival or cell death onset. When the damage is too severe, excitotoxicity due to excessive influx of calcium ions causes neuronal cell death. However, in less damaging situations where calcium levels are appropriately controlled, this triggers proteolysis and membrane fusion/fission processes associated with axonal repair and cytoskeleton reorganization. First, local resealing is a critical early response for regrowth and this requires calcium activation of calpains to cleave the spectrin network and release membrane tension. This might explain why *Capn3* was up-regulated, whereas *Spnb* gene expression was varied. Secondly, calcium is a fundamental co-factor for cytoskeletal remodelling as it is required for membrane vesicle fusion processes used in the delivery of constructive molecules and neurotrophic factors to axotomized ends for resealing purposes and growth cone formation [57]. Varied gene expression of calcium signalling associated genes, and the elevated gene expression of motor and machinery proteins involved in membrane vesicle transport and fusion mentioned earlier, further supported this supposition.

In addition, up-regulation of *SNF1/AMPK*, a calcium-activated kinase involve in metabolic stress, showed that energy level regulation after axotomy is important. This is accompanied by the concomitant elevated expression of its upstream activators such as *Il-6* and *Cntf* [58, 59]. Research on the role of *AMPK* in neurons is new but recent studies have shown that *AMPK* activation in neurons is neuroprotective [60, 61]. More recently, plausible roles for *AMPK* in neuronal polarity and axon specification are indicated by its necessity for the maintenance of cell polarity in epithelial cells [62]. In the case of our study, it is possible that energy regulation in response to calcium ion levels could be crucial for the battle against metabolic insults and the re-establishment and/or maintenance of polarity in severed neurons.

Inflammation

Inflammation in response to axotomy as observed from the presence of *Bf, C2, Nrf1* and *Atrn* could result in cell death if not properly regulated [63–65]. cAMP levels which are increased and limited by the activity of adenylate cyclase (*Adcy*) and phosphodiesterase (*Pde*), respectively, could mitigate inflammation [66, 67]. Elevated gene expression of *Adcy*, *Adcyap* and *Gpr*, but decreased expression of *Pde*, as per our study, clearly suggested that cAMP elevation was adopted to ease inflammation caused by axotomy. More important, increased levels of cAMP were found to promote axonal regeneration and recovery after CNS injury [68]. The likely mechanism for this is increasing the translocation of neurotrophic receptors, for example *NtrkB*, to the plasma membrane of neurons [69]. cAMP could also activate a series of kinases that augment growth promoting signalling pathways in brain and spinal cord injuries [70]. Our data confirm the importance of the role of cellular cAMP level to alleviate inflammation and to push regrowth mechanisms in response to injury. Henceforth, the roles of ATP in *Arp2/3* regulation mentioned earlier, together with the significance of regulating secondary messengers to direct neurite regeneration, highlight the importance of secondary messenger precursors in the study of axonal injury.

Apart from the primary association of cytokines and chemokines with inflammation, they could also directly or indirectly modulate regeneration after injury. This was evident from their robust gene expression profiles. Through a knockout study, *Il6*, a cytokine, was found to promote re-growth of dorsal column axons after static nerve injury [71]. Changes in cytokine levels often alter expression of transcription factors involved in inflammation and regeneration. *Stat3* is one such example and its activation in axons upon injury could act as a retrograde signalling factor to promote regeneration of sensory and motor neurons [72]. As for chemokines, *Cxcr4* for instance, was implicated with neuronal regeneration because it could regulate axonal path finding in the CNS [73]. Notably, *Il6r*, *Stat3* and *Cxcr4* were all transcriptionally up-regulated in our study. These examples highlight the direct impact cytokines and chemokines can have upon regenerating neurons.

Neurite cytoskeleton	
• Microtubule stabilization	↓Cspg, ↓Map, ↑Notch, ↓Stmn, ↓Spg, ↑Tekt, ↑Tub
• Actin filaments dynamics	↓Act, ↓Arpc, ↑Gas, ↑N-WASP, ↓Pfn, ↑PRKCQ, ↑Vil
• Protein trafficking	↑Dnc, ↑Dna, ↑↓Kif, ↑↓Myh, ↓Stx, ↑Snap (8hr), ↑↓Syt, ↑↓Tpm, ↑Vamp
• Repulsive guidance cues and receptors	↓Bmp, ↓Efn, ↑↓Eph, ↓Nrp, ↓Plxdc, ↑↓Plxn, ↓Sema, ↓Slit
• Neurite promoting factors	↑Apoe, ↑Bdnf (8hr), ↑Cntf, ↑Lama, ↓Ngfr, ↓Ntf, ↑Ntrk (8hr), ↑Vgf
Oxidative Stress	
• GSH sythesis	↑Gss, ↑Gstm, ↑Mgst
• Antioxidant enzymes	↑Gpx, ↑Prdx, ↑Sod, ↑↓Txnrd
• Clearance of protein aggregates	↑Hsp, ↑Hspbp
Apoptosis and cell cycle	
• Cell death elusion	↓Apaf, ↓Bid, ↓Bnip, ↑Braf, ↓Casp, ↑Rap
• Alternate neuronal function	↑Aurkb (?), ↓Klf, others (?)
Calcium homeostatsis	
• Axonal resealing	↑Capn, ↑↓Spn (8 & 15hr), ↑S100a1, ↑↓Syt, ↑Vamp
• Energy regulation	↑Cntf, ↑Il, ↑SNF1/AMPK
Inflammatory responses	
• Inflammation	↑Atrn, ↑Bf, ↑C2, ↑Ncf
• Elevated cAMP	↑Adcy, ↑↓Adcyap, ↑Gpr, ↓Pde (except 8hr), ↑Rapgef
Chemotaxis	
• Chemokines	↑↓Ccl, ↑↓Cxcl, ↑Cxcr, ↑Cx3cl1, ↑Cklf
• Cytokines	↑Il, ↑Ilr
• Cytokines induced transcriptional factors	↑c-fos, ↑Stat

Fig. 3 Summarized view on the regulation of selected genes (taken from gene profiles) that were involved in different major sub-processes associated with neurite regeneration after axonal injury *in vitro* as discussed.

Physiologically however, cytokines and chemokines released upon neuroinflammation often have an indirect effect on neurons whereby they help to recruit immune-response cells to injured site. Most of these cells when recruited excessively to injured site could result in neuronal apoptosis but during regeneration, they could also secrete bioactive forms of neurotrophic factors that would potentially aid in neurons' axon regrowth [74–76]. Supplementation of neurite promoting factors by immune cells could possibly explain the transient need for neurons to express their own, such as *Ntrk* and *Bdnf* found in our *in vitro* injury model. Intriguingly, a study showed that oncomodulin secreted by inflammation-activated macrophages could promote axon regeneration in RGCs only upon elevated cAMP levels [77]. It was speculated that increased cAMP caused translocation of specific receptors to the cell surface membrane. Even though this was observed in RGCs, the general idea may still apply for neurons in which they are probably programmed to modulate cellular second messenger levels, such as cAMP, during injury to elicit actions. For example, relocation of specific receptors to the cell membrane in anticipation of binding to neurite-promoting factors released by surrounding immune-response cells.

Conclusion

It is significant that a number of genes listed in our DNA microarray study were in accordance with findings from previous *in vitro* and *in vivo* regenerative studies reported by other groups in relation to spinal cord and brain injuries. This provides affirmation that our protocol of severing axonal bundles *in vitro* to study injury-induced neurite regeneration is a reasonable and valid experimental model. From a transcriptomic view, we have revealed that neurite regeneration is a complex process that mainly involves restructuring of neurite cytoskeleton, determined by intricate actin and microtubule dynamics, protein trafficking and appropriate control of both guidance cues and neurotrophic factors. We conclude that the molecular response of neurons to axotomy is not a simple process and evokes two distinct pathways; a cell survival response accompanied by activation of genes to protect against oxidative stress, inflammation and cellular ion imbalance and a regenerative response driven by modulation of the neuronal cytoskeleton. Gene expression profiles from

our study demonstrated that injured neurons have an innate capability to survive axotomy by elevating biological antioxidants and molecular chaperones, regulating secondary messengers, suppressing apoptotic genes, controlling calcium ion-associated processes and possibly by expressing certain cell cycle proteins which might serve unique alternate neuronal functions. Genes involved in these highlighted protective and regenerative mechanics were summarized in Figure 3. Transcriptional analysis is a powerful and effective screening method to globally search for comprehensive clues to determine which biological pathways are involved in the intrinsic response of neurons to axotomy. Appropriate manipulation of selected biological targets involved in these pathways could then potentially facilitate the design and development of novel, effective therapeutics for axonal damage in CNS injury.

Acknowledgements

This work was financially supported by Singapore Biomedical Research Council research grant R-184-000-093-305, Singapore National Medical Research Council research grant R-183-000-075-213, Strategic Initiative Funding (Menzies Research Institute), National Health and Medical Research Council (AUSTRALIA) research grant 544913, Australian Research Council research grants DP0984673 and DP0556630 and a research grant from the Motor Accident & Insurance Board of Tasmania.

Conflict of interest

There are no conflicts of interest.

References

1. **David S, Aguayo AJ.** Axonal regeneration after crush injury of rat central nervous system fibres innervating peripheral nerve grafts. *J Neurocytol*. 1985; 14: 1–12.
2. **Sandvig A, Berry M, Barrett LB, *et al.*** Myelin-, reactive glia-, and scar-derived CNS axon growth inhibitors: expression, receptor signaling, and correlation with axon regeneration. *Glia*. 2004; 46: 225–51.
3. **Taylor AM, Blurton-Jones M, Rhee SW, *et al.*** A microfluidic culture platform for CNS axonal injury, regeneration and transport. *Nat Methods*. 2005; 2: 599–605.
4. **Taylor AM, Berchtold NC, Perreau VM, *et al.*** Axonal mRNA in uninjured and regenerating cortical mammalian axons. *J Neurosci*. 2009; 29: 4697–707.
5. **Dickson TC, Adlard PA, Vickers JC.** Sequence of cellular changes following localized axotomy to cortical neurons in glia-free culture. *J Neurotrauma*. 2000; 17: 1095–103.
6. **Chuckowree JA, Vickers JC.** Cytoskeletal and morphological alterations underlying axonal sprouting after localized transection of cortical neuron axons *in vitro*. *J Neurosci*. 2003; 23: 3715–25.
7. **Sengottuvel V, Leibinger M, Pfreimer M, *et al.*** Taxol facilitates axon regeneration in the mature CNS. *J Neurosci*. 2011; 31: 2688–99.
8. **Verma P, Chierzi S, Codd AM, *et al.*** Axonal protein synthesis and degradation are necessary for efficient growth cone regeneration. *J Neurosci*. 2005; 25: 331–42.
9. **McCurley AT, Callard GV.** Time course analysis of gene expression patterns in zebrafish eye during optic nerve regeneration. *J Exp Neurosci*. 2010; 2010: 17–33.
10. **Veldman MB, Bemben MA, Thompson RC, *et al.*** Gene expression analysis of zebrafish retinal ganglion cells during optic nerve regeneration identifies KLF6a and KLF7a as important regulators of axon regeneration. *Dev Biol*. 2007; 312: 596–612.
11. **Kuo LT, Tsai SY, Groves MJ, *et al.*** Gene expression profile in rat dorsal root ganglion following sciatic nerve injury and systemic neurotrophin-3 administration. *J Mol Neurosci*. 2010; 43: 503–15.
12. **Vega-Avelaira D, Geranton SM, Fitzgerald M.** Differential regulation of immune responses and macrophage/neuron interactions in the dorsal root ganglion in young and adult rats following nerve injury. *Mol Pain*. 2009; 5: 70.
13. **Di Giovanni S, Faden AI, Yakovlev A, *et al.*** Neuronal plasticity after spinal cord injury: identification of a gene cluster driving neurite outgrowth. *FASEB J*. 2005; 19: 153–4.
14. **Zai L, Ferrari C, Subbaiah S, *et al.*** Inosine alters gene expression and axonal projections in neurons contralateral to a cortical infarct and improves skilled use of the impaired limb. *J Neurosci*. 2009; 29: 8187–97.
15. **Chung RS, Vickers JC, Chuah MI, *et al.*** Metallothionein-III inhibits initial neurite formation in developing neurons as well as postinjury, regenerative neurite sprouting. *Exp Neurol*. 2002; 178: 1–12.
16. **Chung RS, Staal JA, McCormack GH, *et al.*** Mild axonal stretch injury *in vitro* induces a progressive series of neurofilament alterations ultimately leading to delayed axotomy. *J Neurotrauma*. 2005; 22: 1081–91.
17. **Dennis G Jr, Sherman BT, Hosack DA, *et al.*** DAVID: database for annotation, visualization, and integrated discovery. *Genome Biol*. 2003; 4: R60.
18. **Huang da W, Sherman BT, Lempicki RA.** Systematic and integrative analysis of large gene lists using DAVID bioinformatics resources. *Nat Protoc*. 2009; 4: 44–57.
19. **Frank CL, Tsai LH.** Alternative functions of core cell cycle regulators in neuronal migration, neuronal maturation, and synaptic plasticity. *Neuron*. 2009; 62: 312–26.
20. **Hellal F, Hurtado A, Ruschel J, *et al.*** Microtubule stabilization reduces scarring and causes axon regeneration after spinal cord injury. *Science*. 2011; 331: 928–31.
21. **Ferrari-Toninelli G, Bonini SA, Bettinsoli P, *et al.*** Microtubule stabilizing effect of notch activation in primary cortical neurons. *Neuroscience*. 2008; 154: 946–52.
22. **Lowery LA, Van Vactor D.** The trip of the tip: understanding the growth cone machinery. *Nat Rev Mol Cell Biol*. 2009; 10: 332–43.
23. **Korobova F, Svitkina T.** Arp2/3 complex is important for filopodia formation, growth cone motility, and neuritogenesis in neuronal cells. *Mol Biol Cell*. 2008; 19: 1561–74.
24. **Kim YS, Furman S, Sink H, *et al.*** Calmodulin and profilin coregulate axon outgrowth in *Drosophila*. *J Neurobiol*. 2001; 47: 26–38.
25. **Pinyol R, Haeckel A, Ritter A, *et al.*** Regulation of N-WASP and the Arp2/3

complex by Abp1 controls neuronal morphology. *PLoS One*. 2007; 2: e400.
26. **You JJ, Lin-Chao S.** Gas7 functions with N-WASP to regulate the neurite outgrowth of hippocampal neurons. *J Biol Chem*. 2010; 285: 11652–66.
27. **Goley ED, Welch MD.** The ARP2/3 complex: an actin nucleator comes of age. *Nat Rev Mol Cell Biol*. 2006; 7: 713–26.
28. **Fawcett J, Pawson T.** Signal transduction. N-WASP regulation-the sting in the tail. *Science*. 2000; 290: 725–6.
29. **Medeiros NA, Burnette DT, Forscher P.** Myosin II functions in actin-bundle turnover in neuronal growth cones. *Nat Cell Biol*. 2006; 8: 215–26.
30. **Lee JH, Gleeson JG.** The role of primary cilia in neuronal function. *Neurobiol Dis*. 2010; 38: 167–72.
31. **Myers KA, Tint I, Nadar CV, *et al.*** Antagonistic forces generated by cytoplasmic dynein and myosin-II during growth cone turning and axonal retraction. *Traffic*. 2006; 7: 1333–51.
32. **Song XY, Li F, Zhang FH, *et al.*** Peripherally-derived BDNF promotes regeneration of ascending sensory neurons after spinal cord injury. *PLoS One*. 2008; 3: e1707.
33. **Harris NG, Mironova YA, Hovda DA, *et al.*** Pericontusion axon sprouting is spatially and temporally consistent with a growth-permissive environment after traumatic brain injury. *J Neuropathol Exp Neurol*. 2010; 69: 139–54.
34. **Hollis ER II, Jamshidi P, Low K, *et al.*** Induction of corticospinal regeneration by lentiviral trkB-induced Erk activation. *Proc Natl Acad Sci U S A*. 2009; 106: 7215–20.
35. **Montolio M, Messeguer J, Masip I, *et al.*** A semaphorin 3A inhibitor blocks axonal chemorepulsion and enhances axon regeneration. *Chem Biol*. 2009; 16: 691–701.
36. **Goldshmit Y, McLenachan S, Turnley A.** Roles of Eph receptors and ephrins in the normal and damaged adult CNS. *Brain Res Rev*. 2006; 52: 327–45.
37. **Boyles JK, Zoellner CD, Anderson LJ, *et al.*** A role for apolipoprotein E, apolipoprotein A-I, and low density lipoprotein receptors in cholesterol transport during regeneration and remyelination of the rat sciatic nerve. *J Clin Invest*. 1989; 83: 1015–31.
38. **Jang KJ, Kim MS, Feltrin D, *et al.*** Two distinct filopodia populations at the growth cone allow to sense nanotopographical extracellular matrix cues to guide neurite outgrowth. *PLoS One*. 2010; 5: e15966.
39. **Manthorpe M, Engvall E, Ruoslahti E, *et al.*** Laminin promotes neuritic regeneration from cultured peripheral and central neurons. *J Cell Biol*. 1983; 97: 1882–90.
40. **Dutta R, McDonough J, Chang A, *et al.*** Activation of the ciliary neurotrophic factor (CNTF) signalling pathway in cortical neurons of multiple sclerosis patients. *Brain*. 2007; 130: 2566–76.
41. **Ye J, Cao L, Cui R, *et al.*** The effects of ciliary neurotrophic factor on neurological function and glial activity following contusive spinal cord injury in the rats. *Brain Res*. 2004; 997: 30–9.
42. **Cui Q, Lu Q, So KF, *et al.*** CNTF, not other trophic factors, promotes axonal regeneration of axotomized retinal ganglion cells in adult hamsters. *Invest Ophthalmol Vis Sci*. 1999; 40: 760–6.
43. **Shuto T, Horie H, Hikawa N, *et al.*** IL-6 up-regulates CNTF mRNA expression and enhances neurite regeneration. *Neuroreport*. 2001; 12: 1081–5.
44. **Muchowski PJ, Wacker JL.** Modulation of neurodegeneration by molecular chaperones. *Nat Rev Neurosci*. 2005; 6: 11–22.
45. **Bruey JM, Ducasse C, Bonniaud P, *et al.*** Hsp27 negatively regulates cell death by interacting with cytochrome *c*. *Nat Cell Biol*. 2000; 2: 645–52.
46. **Williams KL, Rahimtula M, Mearow KM.** Hsp27 and axonal growth in adult sensory neurons *in vitro*. *BMC Neurosci*. 2005; 6: 24.
47. **Read DE, Gorman AM.** Heat shock protein 27 in neuronal survival and neurite outgrowth. *Biochem Biophys Res Commun*. 2009; 382: 6–8.
48. **Dubois-Dauphin M, Frankowski H, Tsujimoto Y, *et al.*** Neonatal motoneurons overexpressing the bcl-2 protooncogene in transgenic mice are protected from axotomy-induced cell death. *Proc Natl Acad Sci U S A*. 1994; 91: 3309–13.
49. **Shibata M, Murray M, Tessler A, *et al.*** Single injections of a DNA plasmid that contains the human Bcl-2 gene prevent loss and atrophy of distinct neuronal populations after spinal cord injury in adult rats. *Neurorehabil Neural Repair*. 2000; 14: 319–30.
50. **Kruman, II, Wersto RP, Cardozo-Pelaez F, *et al.*** Cell cycle activation linked to neuronal cell death initiated by DNA damage. *Neuron*. 2004; 41: 549–61.
51. **Fuller BG, Lampson MA, Foley EA, *et al.*** Midzone activation of aurora B in anaphase produces an intracellular phosphorylation gradient. *Nature*. 2008; 453: 1132–6.
52. **Murata-Hori M, Wang YL.** The kinase activity of aurora B is required for kinetochore-microtubule interactions during mitosis. *Curr Biol*. 2002; 12: 894–9.
53. **Khazaei MR, Puschel AW.** Phosphorylation of the par polarity complex protein Par3 at serine 962 is mediated by aurora a and regulates its function in neuronal polarity. *J Biol Chem*. 2009; 284: 33571–9.
54. **Yamada M, Hirotsune S, Wynshaw-Boris A.** The essential role of LIS1, NDEL1 and Aurora-A in polarity formation and microtubule organization during neurogensis. *Cell Adh Migr*. 2010; 4: 180–4.
55. **Rowland BD, Peeper DS.** KLF4, p21 and context-dependent opposing forces in cancer. *Nat Rev Cancer*. 2006; 6: 11–23.
56. **Moore DL, Blackmore MG, Hu Y, *et al.*** KLF family members regulate intrinsic axon regeneration ability. *Science*. 2009; 326: 298–301.
57. **Hay JC.** Calcium: a fundamental regulator of intracellular membrane fusion? *EMBO Rep*. 2007; 8: 236–40.
58. **Kelly M, Gauthier MS, Saha AK, *et al.*** Activation of AMP-activated protein kinase by interleukin-6 in rat skeletal muscle: association with changes in cAMP, energy state, and endogenous fuel mobilization. *Diabetes*. 2009; 58: 1953–60.
59. **Escartin C, Pierre K, Colin A, *et al.*** Activation of astrocytes by CNTF induces metabolic plasticity and increases resistance to metabolic insults. *J Neurosci*. 2007; 27: 7094–104.
60. **Dasgupta B, Milbrandt J.** Resveratrol stimulates AMP kinase activity in neurons. *Proc Natl Acad Sci U S A*. 2007; 104: 7217–22.
61. **Spasic MR, Callaerts P, Norga KK.** AMP-activated protein kinase (AMPK) molecular crossroad for metabolic control and survival of neurons. *Neuroscientist*. 2009; 15: 309–16.
62. **Williams T, Brenman JE.** LKB1 and AMPK in cell polarity and division. *Trends Cell Biol*. 2008; 18: 193–8.
63. **Zipfel PF, Lauer N, Skerka C.** The role of complement in AMD. *Adv Exp Med Biol*. 2010; 703: 9–24.
64. **Gupta-Bansal R, Parent JB, Brunden KR.** Inhibition of complement alternative pathway function with anti-properdin monoclonal antibodies. *Mol Immunol*. 2000; 37: 191–201.
65. **Hultqvist M, Sareila O, Vilhardt F, *et al.*** Positioning of a polymorphic quantitative trait nucleotide in the Ncf1 gene controlling oxidative burst response and arthritis severity in rats. *Antioxid Redox Signal*. 2011; 14: 2373–83.

66. **Silveira MS, Linden R.** Neuroprotection by cAMP: another brick in the wall. *Adv Exp Med Biol*. 2006; 557: 164–76.
67. **Ohta A, Sitkovsky M.** Role of G-protein-coupled adenosine receptors in downregulation of inflammation and protection from tissue damage. *Nature*. 2001; 414: 916–20.
68. **Spencer T, Filbin MT.** A role for cAMP in regeneration of the adult mammalian CNS. *J Anat*. 2004; 204: 49–55.
69. **Meyer-Franke A, Wilkinson GA, Kruttgen A, *et al.*** Depolarization and cAMP elevation rapidly recruit TrkB to the plasma membrane of CNS neurons. *Neuron*. 1998; 21: 681–93.
70. **Cui Q, So KF.** Involvement of cAMP in neuronal survival and axonal regeneration. *Anat Sci Int*. 2004; 79: 209–12.
71. **Cafferty WB, Gardiner NJ, Das P, *et al.*** Conditioning injury-induced spinal axon regeneration fails in interleukin-6 knockout mice. *J Neurosci*. 2004; 24: 4432–43.
72. **Lee N, Neitzel KL, Devlin BK, *et al.*** STAT3 phosphorylation in injured axons before sensory and motor neuron nuclei: potential role for STAT3 as a retrograde signaling transcription factor. *J Comp Neurol*. 2004; 474: 535–45.
73. **Stumm R, Hollt V.** CXC chemokine receptor 4 regulates neuronal migration and axonal pathfinding in the developing nervous system: implications for neuronal regeneration in the adult brain. *J Mol Endocrinol*. 2007; 38: 377–82.
74. **Elkabes S, DiCicco-Bloom EM, Black IB.** Brain microglia/macrophages express neurotrophins that selectively regulate microglial proliferation and function. *J Neurosci*. 1996; 16: 2508–21.
75. **Kerschensteiner M, Gallmeier E, Behrens L, *et al.*** Activated human T cells, B cells, and monocytes produce brain-derived neurotrophic factor *in vitro* and in inflammatory brain lesions: a neuroprotective role of inflammation? *J Exp Med*. 1999; 189: 865–70.
76. **Nakajima K, Honda S, Tohyama Y, *et al.*** Neurotrophin secretion from cultured microglia. *J Neurosci Res*. 2001; 65: 322–31.
77. **Yin Y, Henzl MT, Lorber B, *et al.*** Oncomodulin is a macrophage-derived signal for axon regeneration in retinal ganglion cells. *Nat Neurosci*. 2006; 9: 843–52.